

AGATA: Performance of γ -ray tracking and associated algorithms

F.C.L. Crespi¹, J. Ljungvall^{*2}, A. Lopez-Martens², and C. Michelagnoli³

¹Dipartimento di Fisica, Università degli Studi di Milano, I-20133 Milano, Italy, and, INFN Sezione di Milano, I-20133 Milano, Italy

² Université Paris-Saclay, CNRS/IN2P3, IJCLab, 91405 Orsay, France

³ Institut Laue-Langevin, 71 Avenue des Martyrs, 38042 Grenoble, France

Received: date / Accepted: date

Abstract

AGATA is a modern γ -ray spectrometer for in-beam nuclear structure studies, based on γ -ray tracking. Since more than a decade, it has been operated performing experimental physics campaigns in different international laboratories (LNL, GSI, GANIL). This paper reviews the obtained results concerning the performances of γ -ray tracking in AGATA and associated algorithms. We discuss γ -ray tracking and algorithms developed for AGATA. Then, we present performance results in terms of efficiency and peak-to-total for AGATA. The importance of the high effective angular resolution of γ -ray tracking arrays is emphasised, e.g. with respect to Doppler correction. Finally, we briefly touch upon the subject of γ -ray imaging and its connection to γ -ray tracking.

Keywords AGATA — Gamma-ray spectroscopy — Gamma-ray tracking — Gamma-ray imaging

PACS 29.40.Wk Solid-state detectors, 29.30.-h Spectrometers and spectroscopic techniques

1 Introduction

The Advanced GAMMA Tracking Array (AGATA) [1] is the European state-of-the-art high-resolution γ -ray spectrometer. A similar project in the US is called

^{*}Corresponding author: joa.ljungvall@ijclab.in2p3.fr

GRETINA/GRETA [2, 3]. In past decades, developments in the technology of semiconductor (HPGe) detectors resulted in, systematically, to significant advancements in nuclear science. In fact, since the first generation of large arrays of HPGe detectors (~ 1981) became available, high-resolution spectroscopic experiments played a primary role in illuminating fundamental aspects of nuclear structure. With the second generation arrays, based on Compton-suppressed HPGe detectors (e.g. GAMMASPHERE, EUROBALL), this technology reached a saturation point in terms of experimental sensitivity for in-beam high-resolution γ spectroscopy studies (see e.g. Lee et al. [4] and Eberth et al. [5]). It was then realised that the possibility to overcome this technological limit was given by being able to produce new HPGe detectors featuring millimetric position resolution, obtained through the physical segmentation of the detector electrode and the analysis of the shapes of the electric signals. This kind of segmented HPGe detectors allows, in fact, to reconstruct the path of a γ ray that interacted in their active volume. In terms of experimental sensitivity advantages, the γ -ray tracking technology permits, for example, to maximise the detection efficiency (due to the elimination of the Compton shields), and to recover the energy resolution degradation due to the Doppler effect. This while retaining a good suppression of radiation not coming from the target position. These features fit specific needs of in-beam high-resolution γ spectroscopy experiments with radioactive beams, that are at the forefront of present nuclear structure research.

The AGATA array is designed to be composed of 180 36-fold segmented HPGe detectors, grouped in 60 triple clusters (final configuration), resulting in a coverage of 80% of 4π of solid angle around the target position. In the present phase of the project a coverage of 1π solid angle has been reached, corresponding to 15 AGATA Triple Clusters (ATCs). Recently a Memorandum of Understanding was signed between the different partner institutes for a phase 2 of the project, bringing the array up to a solid coverage of 3π in 2030. In this manuscript we review the performance of the γ -ray tracking in AGATA, referring also to specific opportunities of accessing novel experimental physics information as compared with previous generation HPGe arrays. In the initial phase of the AGATA project the performances of γ -ray tracking were extensively studied via Geant4 simulations [6].

Presently, after about 12 years of operation in experimental physics campaigns in different international laboratories (LNL, GSI, GANIL), these performances can be highlighted with reference to many experimental results, as it will be shown in the following. For a recent review of the scientific output and perspectives of AGATA, see e.g. [7, 8].

2 General considerations for γ -ray tracking

Since Compton scattering is the dominant interaction mechanism of photons in Ge for energies ranging from 150 keV to 10 MeV, tracking algorithms are mainly based on the properties of the Compton interaction process.

In particular, they rely on the following relationship between incident E_{i-1} and scattered E_i energies and scattering angle θ_i (assuming that the electrons of the Ge detectors are at rest):

$$\cos(\theta_i) = 1 - m_e c^2 \left(\frac{1}{E_i} - \frac{1}{E_{i-1}} \right) \quad (1)$$

Most tracking algorithms attempt to reconstruct the tracks of photons, which have been fully absorbed in the Ge detectors (there is the notable exception of the TANGO algorithm [9], which also identifies Compton escape events, see section 4). There are two categories of tracking algorithms: forward-tracking algorithms [10], which start from the known position of the source and reconstruct the track of photons as they interact in the detector and back-tracking algorithms [11], which start from the potential photoelectric interaction point and reconstruct the track backwards to the source. Forward-tracking algorithms have been demonstrated to be more efficient than back-tracking algorithms [12] and are therefore used both at AGATA [1] and GREY [13].

Three algorithms have been used to track AGATA data: The Mars Gamma Tracking algorithm [14] (MGT) and the Orsay Forward Tracking algorithm [12] (OFT), which are both implemented into the AGATA data acquisition software, and the Gretina Tracking algorithm [15, 16] (henceforth called GT). These algorithms are composed of two parts: the first one consists in defining a pool of clusters of interaction points in 3-dimensional space and the second part consists in finding the best sequence of interaction points for each cluster and keeping only those sequences, whose figure of merit lies above a given threshold.

The clusterisation of points is typically performed on the basis of the angular separation between points. The free parameter is then the maximum opening angle, as is the case in GT. For OFT and MGT, the maximum angle depends on the number of interaction points detected in each event and is therefore not a tuneable parameter. Other more sophisticated clusterisation algorithms have been developed in the framework of AGATA, such as the fuzzy C-means algorithm [17] (see section 4) or the Deterministic Annealing Filter [18]).

The evaluation of clusters containing more than one interaction point then proceeds as follows: starting from the known position of the source, and assuming that the total deposited energy in a cluster corresponds to the energy of an incident photon, the figure of merit of every possible sequence of interaction points within the cluster is computed by evaluating the goodness of each vertex in the sequence by comparing the measured energies and angles with the corresponding quantities obtained via equation 1. As shown in Fig. 1 this comparison can be performed in different ways.

GT uses the last comparator V_i^θ of Figure 1, while OFT and MGT use the first comparator V_i^E with an added weight, which accounts for range and interaction-process probabilities in going from interaction-point $i-1$ to i and $i+1$. A weighted square sum of these vertices is used by MGT while OFT uses a likelihood like formulation. For OFT, the comparator V_i^E is also weighted by the

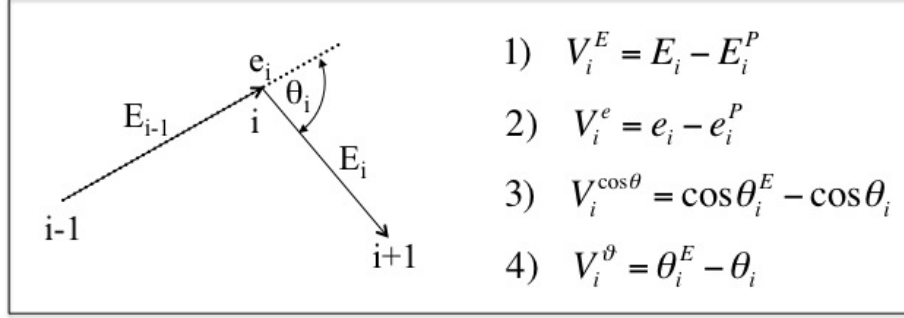


Figure 1: Example of a Compton scattering vertex, in which an incident photon of energy E_{i-1} , deposits the energy e_i at vertex i and is scattered at an angle θ_i with energy E_i . The superscript P indicates scattered and deposited energies obtained through measured interaction-point (or source) positions and the superscript E indicates angles or cosines calculated from the measured deposited energies.

associated experimental uncertainties in the deposited energies and interaction positions.

The evaluation of single-interaction-point “clusters” is an important part of all tracking algorithms since the efficiency loss when it is not included is very large for low energy events, and non-negligible at higher energies. As a consequence of how the Pulse Shape Analysis (PSA) algorithm (Adaptive Grid Search [19]) identifies interaction points in AGATA, $\sim 20\%$ of 1.4 MeV total-absorption events in AGATA detectors are found in single interaction points. This is at variance with the situation at GRETINA, where the signal decomposition algorithm allows for more than one hit per segment, and the number of single-interaction points is found to be less than what is expected from Geant4 [20] simulations (see Tab. 6 of ref. [15]). How single-interaction clusters are selected and validated depends on the algorithm, but the common criterion to accept or reject the cluster is the depth of the interaction point inside the AGATA detectors.

2.1 Limiting factors

Physics imposes some limits on γ -ray tracking:

1. The electron generated by the Compton scattering will deposit its energy in a volume of up to several mm^3 . The energy loss proceeds via ionisation and the emission of bremsstrahlung. As a consequence, even with an exact PSA, the Compton relation will not be perfectly fulfilled as the vertex given by PSA is displaced with respect to interaction position.
2. The relation given in equation (1) is only valid when the electrons on

which the γ ray scatters is at rest. This is not the case for electrons in atoms as they have finite momentum, making the relationship between angle and deposited energy an approximation only.

3. Rayleigh scattering of γ rays. As the γ ray does not loose energy but changes direction an uncertainty in the scattering direction is introduced. This happens mainly for low-energy γ rays, i.e. at the end of a track closer to the photo-electric absorption than the resolving power of the PSA. In practice its impact is therefor small on the performance of γ -ray tracking.
4. For tracks with 2 interactions there is an ambiguity for the order of the two interactions.

These limitations lead to an an overlap between the figure of merit for correctly ordered fully absorbed γ rays and not fully absorbed γ rays or wrongly ordered sequences of interaction points. This was recognised early in the AGATA and GRETA projects, e.g. see Milechina et al. [21] discussing the impact of the finite electron momentum and Vetter et al. [22] adding to this the discussion of the finite range of the Compton electron. In the work of Lopez-Martens et al. [12] these effects were simultaneously quantified using Geant4 [20] simulations. The simulations were made assuming a position-resolution of about 2.4 mm FWHM for Milenchina et al. [21] and 5 mm FWHM for Lopez-Martens et al. the [12]. Energy depositions were packed within the assumed position resolution. The conclusion of Lopez-Martens et al. is that both for back-tracking and cluster-based tracking algorithms the major uncertainty in the scattering angle comes from the finite volume in which the Compton electron deposits its energy. Including the energy-loss process of the Compton electron reduced the efficiency for fully detecting 30 1.3 MeV γ rays using the back-tracking method from 23.4% to 21.1%. Including the electron momentum distribution give 21.9% and 21.2%, respectively. This is compatible with what was found by Milechina et al. [21], where the efficiency dropped from 33% to 24% for a multiplicity 25 of 1.3 MeV γ rays when including the electron momentum. The conclusion is that improving the position resolution from PSA (presently around 5 mm FWHM [23, 24, 25]) will improve the γ -ray tracking.

Hammond et al. [26] pointed out that for γ rays with an energy above 255 keV that are absorbed in two interactions, i.e. one Compton scattering followed by a photo-electric absorption, there is an ambiguity in the order of the two interaction points. In theory this is most troublesome for γ rays with in the energy range of 500-700 keV. In AGATA, that assumes one interaction point per segment, this ambiguity is found in a larger energy range and introduces an uncertainty in the ordering of the interaction points.

3 Gamma-ray tracking algorithms implemented in AGATA

The γ -ray tracking algorithms that are used in the AGATA collaboration have been described in a recent review by Korichi and Lauritsen [16]. For this reason we will only give an description of the major changes to the OFT code since then. For other γ -ray tracking codes and algorithms that are or have been in use with the AGATA community we only provide short descriptions with the appropriate references as no significant development has been made.

3.1 OFT

The original OFT code is described in reference [12]. In this section, we will detail the recent modifications to the code.

3.1.1 Distance calculation

To compute the ranges of photons in Ge, effective distances in Ge between interaction points as well as the effective distance between every interaction point and the position of the source need to be calculated. The problem can be solved geometrically if one approximates the detector geometry to a shell of Ge of inner radius R_0 . This approximation was checked with the Geant4 AGATA simulation code [6], in which the exact geometry of AGATA is defined, i.e. the shape of the crystals, the encapsulations, the cryostats, the empty spaces and the distances between all these elements. The efficiency and P/T were found to be the same at 1.3 MeV using the exact distances as compared to using distances obtained via the shell approximation. However, the approximation leads to an overestimation of the distance travelled by photons from the source into the detector by up to a few mm. The extra distance travelled is greatest for interactions situated at large radii in the detectors. This overestimation is extremely penalising for low-energy photons (<60 keV), which have very small ranges in Ge and are therefore awarded a poor range probability by OFT. A correction has been added to the distance calculation routine in the OFT algorithm. Figure 2 shows the resulting improvement of the tracked efficiency at low energy. For a more in depth discussion of “tracking” at very low energies, see Section 5.2.

3.1.2 Cluster search

Points are clusterised according to their relative angular distance. If the relative angular separation between interaction point i and any other interaction point is larger than α , i is assigned to a single interaction cluster. For a given value of α , no interaction point can be assigned to more than 1 cluster. This clusterisation is repeated for various values of α . The span of α depends on the total number of interaction points in the event nb_int :

$$\alpha_{max} = \text{acos}(1 - \frac{2}{((nb_int + 2)/3)^{0.9}}) \quad (2)$$

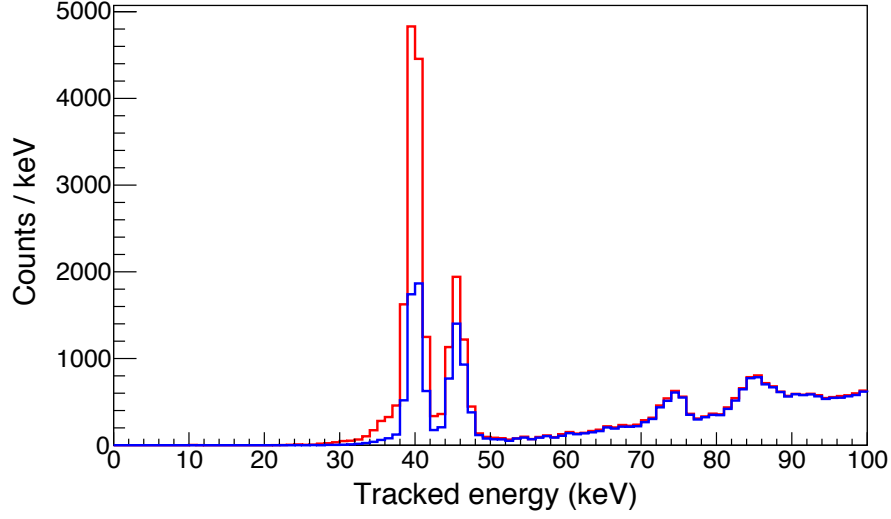


Figure 2: Comparison of the low-energy part of a tracked spectrum of γ rays emitted by a ^{152}Eu source with the usual sphere approximation (blue) and correcting for the overestimation of the effective distances travelled in Ge (red). The gain in efficiency at 40 keV is close to factor 3. The data was taken at GANIL.

The introduction of a dependence of the maximum allowed value of α on the number of interaction points in the event was fine-tuned with simulated data for MGT. For OFT, including such a dependence in the code resulted in an increase of the simulated efficiency and peak-to-total for low and medium γ -ray multiplicities and a slight improvement of the tracking performance at high multiplicities. A new feature has recently been added to the code, namely the possibility to reduce α_{max} by a factor to be fine-tuned by the user. As an example, reducing α_{max} increases the efficiency to track 100-300 keV γ rays for events with a small number of interaction points.

3.1.3 Cluster evaluation

Compton events

In OFT, the figure of merit L of a particular sequence of n interaction points is given by:

$$L^{2n-1} = \prod_{i=1}^{n-1} P_i \exp^{-a \left(\frac{V_i^E}{\sigma_E} \right)^2} \quad (3)$$

where i is the Compton vertex number, P_i contains the physics information regarding interaction probabilities at i and $i+1$ and ranges in Ge to and from i ,

a is 2 at $i = 1$ and 1 for $i > 1$ and σ_E is the uncertainty in the determination of the scattered energies due to the uncertainty in the determination of interaction-point energy depositions as well as positions. The average position uncertainty is parameterized by a free parameter σ_θ in cm and it enters in the calculation of σ_E . Until the availability of data from AGATA, OFT was developed with simulated data sets produced with the AGATA simulation code (see Farnea et al. [6] and Labiche et al. [27] in this issue). The output of the simulations was modified to mock the expected experimental conditions, such as energy resolution and threshold and position resolution. To reproduce the experimental position resolution, interaction points were packed together if they happened to be in the same segment of the same detector and their positions smeared in x, y and z using a Gaussian distribution of full width at half maximum (FWHM) :

$$FWHM(cm) = S_0 \times \sqrt{\frac{0.1}{e_i}} \quad (4)$$

where e_i is the energy of interaction point i in MeV and S_0 was taken to be 0.5 cm. The optimal parameters of the algorithm were tuned in such a way as to maximise the product of efficiency and P/T and the best tracking performance was obtained with $\sigma_\theta=0.24$ cm in the case of 1 MeV incident photons [12]. The experimentally-determined value of S_0 [24] turns out to be larger and this explains why with real source and in-beam data, the optimal parameter σ_θ was extracted to be 0.8 cm. It was also found that setting $a=2$ for the first Compton vertex in the track reduces the performance of OFT compared to what was obtained with simulated data and so now a is set to 1 for all vertices.

Pair-production events

To increase the tracking efficiency at high energy, it is necessary to track pair-production events since for photon energies above 10 MeV, pair-production is the dominant physical interaction process in Ge. However, it must be considered that including pair production becomes important already at γ -ray energies significantly lower than 10 MeV, since we are interested only in full energy peak events. The pattern that is tracked is the one in which a cluster contains an interaction point collecting the incident photon energy E_γ minus twice the electron rest-mass.

The total-absorption events of this type represent $\sim 60\%$ of the total-absorption pair-production events for 2 MeV incident photons (see Fig. 3). This number decreases steadily as the incident photon energy increases to reach roughly 20% at 10 MeV. This decrease is due to the increase in energy transferred to the electron-positron pair, which results in a less localised deposition of energy around the position of the pair-production interaction point. However, this type of event represents a growing fraction of the overall total absorption events (2% at 2 MeV, 10% at 4 MeV and close to 15% at 10 MeV). This trend is related to the increase of the pair-production cross-section with increasing incident photon energy. To accommodate for pair-production clusters, the maximum number of

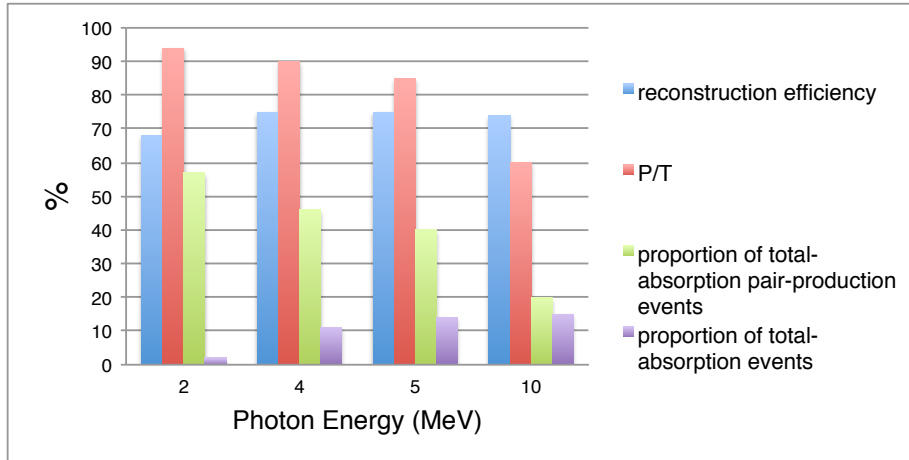


Figure 3: Reconstruction efficiency and P/T of the pair-production tracking routine as a function of incident photon energy. The fractions of the pair-production and overall events resulting in total absorption, which can, in principle, be tracked are also shown. Data from geant4 simulations of HPGGe shell and treated as in Lopez-Martens et al. [12].

allowed interaction points in the clusterisation procedure has been increased from 7 to 10, but clusters with more than 7 interaction points are not evaluated as possible Compton events since this deteriorates the global P/T.

If a cluster has an interaction point with an energy corresponding to the total cluster energy minus twice the electron rest-mass it is given the figure of merit equal to the square root of the probability for the incident photon to travel the distance in Ge from the source to the position of the interaction point multiplied by the probability to undergo a pair-production interaction. If this figure of merit is found to be larger than the best Compton sequence, the cluster is flagged as a pair-production event.

As can be seen in Fig. 3, the reconstruction efficiency of such pair-production events is rather high, since it is of the order of 70% for incident photons of energy ranging from 2 to 10 MeV. Furthermore, the number of wrongly recognised pair-production clusters is small: the peak-to-total of the pair-production tracking routine is 85% at 5 MeV, and 60% at 10 MeV. Reconstruction of at least one of the 511 keV annihilation photons did not improve the P/T and led to an overall reduced pair-production tracking efficiency.

Single-interaction events

The evaluation of single-interaction-point clusters is performed after the evaluation of the multi-interaction-point clusters.

One of the criteria for a “clean” identification of a single-interaction point

is that it is well isolated from other hits. The optimal minimal distance to the closest interaction point is found to be 4 cm. If a single-interaction point fits this criterion, the figure of merit of the corresponding cluster is computed. In reference [12], it was defined as the square root of the probability for the incident photon to travel the distance in Ge from the source to the position of the interaction point multiplied by the probability to undergo a photoelectric interaction. Depending on the threshold of acceptance, the spectrum of “tracked” single-interaction clusters had a different end point: ~ 600 keV for a minimum figure of merit of 0.15 and ~ 2 MeV for 0.02. Accepting high-energy single interaction points therefore came at the cost of a large background. The procedure has now been changed and only the range in Ge is considered through an experimentally-defined energy-dependent formula (a second order polynomial expression). This results in a reduction of the background at low energies while preserving the photo peak efficiency.

3.2 Other γ -ray tracking algorithms

- The MGT code [14, 28, 29] was developed in the TMR program “Development of γ -ray tracking detectors”. It was used extensively in the early phase of AGATA.
- The tracking code used by the GRETINA/GRETA [10] collaboration, referred to as GT, has also been tested with AGATA data. The two tracking codes, i.e. OFT and GT, perform very similar with a slight advantage at high γ -ray multiplicities for OFT and at low γ -ray multiplicities for GT [16, 30, 31].
- Although not a part of the official distribution of software of AGATA, the Bayes tracking [32] has been tested on source data, and is included as an algorithm that has been implemented for AGATA. The algorithm formulates the problem of γ -ray tracking, with the help of Bayes theorem, as maximising the probability for the measured set of interaction points given a number of emitted γ rays. This for all possible permutation, for 1 to N γ rays where N is the number interaction points. For such a rigorous mathematical formulation estimation of probabilities for, e.g., the number of interaction for a γ ray of given energy, have to be calculated. This has been done using Geant4 [20] simulations with the standard AGATA code[6], i.e. using packed simulated data with realistic detector geometry. The Bayes tracking algorithm can in principle also reconstruct the γ -ray energy for a not fully absorbed γ ray.

4 Other clustering and γ -ray tracking algorithms

Extensive investigations have been made to try to improve the clustering+validation process used in the MGT, OFT, and GT algorithms. These efforts can be classified in two groups whether it is the clustering or the evaluation of the clusters

that is targeted. The Fuzzy C Logic [17] and the Deterministic Annealing Filter [18] aim at improving the clustering of γ ray interaction points into trail clusters before evaluation. Both have been tried with simulated data giving interesting results. The New tracking ALGOritm for gamma rays (TANGO) [9] introduces more complex figure-of-merits in the cluster evaluation and the possibility to estimate the energy of not fully absorbed γ rays.

A first approach to a self-calibrating γ -ray tracking algorithm, based on experimental data, was presented in [33]. In this paper the influence of non-Gaussian behaviour in scattering angles between three points in 3D-space as well as the impact of PSA-induced interaction point merging on Compton-scattering angles and consecutively on γ -ray tracking with AGATA have been discussed. Although the algorithm was tested with ^{137}Cs source data, for its application in real experimental conditions and for having a thorough comparison with the performances of OFT tracking, the study still needs completion. Gamma-ray tracking was used in the work by Heil et al. [34] to experimentally determine a pulse-shape data base for PSA. Pulse-shapes from experimental data are grouped together into collections of hits, based on their pulse shapes. Each hit collection is then given a position. All the hits inside a hit collection are then linked to the hits in the other hit collections. The positions for the hit collections are then varied to maximise the Figure-Of-Merit, corresponding to γ -ray tracking of the linked hits. As each hit collection contains many different hits linked to other hits the location of the hit collections have well optimal positions. The optimisation procedure is performed in an iterative manner. It has to date only been tested on simulated data using the actual positions of the interaction as the criteria to create the hit collections. Efforts to test the method with experimental data and pulse-shapes are ongoing (end of year 2022).

Andersson and Bäck [35] have recently investigated the use of graph neural networks for γ -ray tracking. This exploratory work based on Geant4 simulations produced very encouraging results where the neural network based tracking outperforms both forward tracking and back tracking on simulated data. In the simulations an ideal 4π Ge shell was used.

5 Performance of γ -ray tracking in AGATA

The performance of AGATA has been continuously evaluated since its first materialisation as the AGATA demonstrator at Legnaro-INFN Laboratory [36]. These evaluations have focused on Photopeak efficiency (ϵ_{ph}) and the Peak-to-Total (P/T) of both the crystals used as individual detectors and after γ -ray tracking. By looking at both the individual detectors and the final result of γ -ray tracking, and comparing them with Geant4 simulations, it is possible to not only characterise the performance of AGATA but also to find where improvements might be possible. In the following these findings will be discussed individually for three different energy regimes. The “normal energy regime” will be discussed in section 5.1, the “low energy regime” is discussed in section 5.2, and finally the “high-energy regime” in section 5.3.

5.1 Normal γ -ray energy regime ($\approx 100 \text{ keV} < E_\gamma < 5 \text{ MeV}$)

This energy regime is characterised by the dominance of Compton scattering. The pair production mechanism becomes of relevance toward the upper energy boundary of the interval. Tracking of events with energy close to the lower energy boundary is limited by the mean-free path of the γ rays being only a few millimeters and the low signal-to-noise ratio of the pulses not allowing the PSA to identify the interaction positions with high precision.

The performance of AGATA at GSI [37] as well as at GANIL [25] in this energy regime were thoroughly investigated using source measurements. Resulting efficiencies and P/T's were compared with simulations. For the GSI measurements 21 crystals were present, whereas for the GANIL measurements 30 detectors were installed in the array, out of which one was not used for the efficiency measurements. In both works the absolute efficiency after γ -ray tracking were determined using standard γ -ray sources. Lalović et al. used ^{60}Co , ^{152}Eu , and ^{56}Co whereas Ljungvall et al. did not look at the high-energy response given by ^{56}Co . Efficiencies were determined using both singles measurements corrected for dead time as well as coincidence measurements corrected for angular correlations for both the GSI and GANIL setups.

The measured efficiencies after γ -ray tracking at 1.4 MeV are 2.50(2)% and 3.67(1)% for the GSI and GANIL phase, respectively. The P/T for the two cases are 38(1)% and 36(1)% respectively. A linear scaling from 21 to 29 detectors would give an efficiency of 3.5%. However, these efficiency numbers depend on the choice of parameters both for MGT and OFT so the two sets of data taken at different times are indeed compatible with each other. The efficiencies as a function of γ -ray energy are shown in figure 4a for GSI and in figure 4b for GANIL, respectively. In all cases single-interaction events are included.

5.2 Low-energy γ rays ($E_\gamma < 100 \text{ keV}$)

For γ rays with an energy lower than about 100 keV γ -ray tracking is not really applicable as the probability for scattering is very low. Instead the “single interaction validation” procedure is used. As described in section 3.1, this is essentially a test comparing the distance the γ ray has travelled in germanium with an empirical relation deduced from experimental data. For low-energy γ rays it is also important to correctly calculate the path inside the HPGe crystal, as shown in section 3.1 and figure 2.

In the case of very-low energy γ rays and x-rays an additional complication arrives. The very low signal-to-noise ratio gives unreliable PSA - the interaction is therefore often positioned by the PSA much deeper into the crystal than it occurred (this can be evidenced by looking at the depth distribution of interaction points as given by PSA gating on an, e.g., x-ray line in ^{152}Eu using non-tracked data). The single interaction validation procedure will then discard it as a low-angle Compton scattering of a higher energy γ ray. In the case that low-energy efficiency is needed a solution has been proposed in which under certain conditions the PSA result is “corrected” to a value that is compatible with

the mean-free path of a γ ray with the energy of the interaction. For further details see Clément et al.[38].

5.3 High-energy γ rays ($E_\gamma > 5\text{MeV}$)

It is worth mentioning that an idea to improve the performances at high energies, for γ -ray spectrometers based on position sensitive detectors, was already proposed rather long time ago by Glenn Knoll and collaborators [39]. In the case of AGATA, a work of 2013 [40] studied the response of AGATA detectors to γ rays up to 15.1 MeV. Gamma rays up to an energy of ≈ 9 MeV were obtained with an extended Am-Be-Fe source. Then, the only feasible way to have γ lines of even higher energies was to use in-beam reactions (see e.g. [41, 42]). In particular, the reaction $d(^{11}\text{B}, n\gamma)^{12}\text{C}$ at $E_{\text{beam}}=19.1$ MeV was used to produce the 15.1 MeV γ 's. To be noted that in this case the γ 's are emitted in flight by the ^{12}C ions ($\beta \approx 4\%$) and this fact was used to test the Doppler correction capabilities of AGATA at these high energies. The energy resolution of AGATA detectors was found to scale $\propto E^{-1/2}$ up to 9 MeV, as expected (see upper panel of Fig. 5). Also the linearity was studied and the energy-to-pulse-height conversion resulted to be linear within $\sim 0.05\%$ up to the γ energy of 15.1 MeV (see lower panel of Fig. 5).

These data also showed that the application of γ -ray tracking allows some suppression of background caused by n-capture in Ge nuclei. The neutrons, in this case, were emitted by the Am-Be source. This background suppression capability of the tracking software can be directly appreciated observing the disappearance of the 10.196 MeV peak originated indeed from neutron interactions (see Fig. 8 in [40]). The value 10.196 MeV corresponds, in fact, to the sum-energy of the γ 's emitted following the ^{74}Ge nucleus de-excitation (Q-value of the neutron capture reaction).

From the operational point of view, it was important to properly set the AGATA electronics for the detection of high-energy γ rays. Specifically, in order to have the ~ 20 MeV dynamic range also for the segment signals acquisition (normally the ~ 4 MeV range is set). The core, instead, has always two channels in the data acquisition by default, for the ~ 4 MeV and ~ 20 MeV range respectively. The Doppler correction quality, at the very high energy of 15.1 MeV, was found to be consistent with the expectations, according to a dedicated Geant4 simulation (see results reported in in [40]). The main limiting factor in the Doppler correction quality, in this case, was found to be the missed event-by-event reconstruction of the velocity vector of the ^{12}C nucleus. From an extrapolation based on the results presented in [40], an intrinsic resolution of about 10 keV is expected at the γ energy of 15 MeV.

Regarding the tracking performances (MGT algorithm was used) at 15 MeV, it was found more convenient to use the so-called calorimeter mode, for getting the non-Doppler corrected energy of an event, and then use the position of the most energetic hit given by the PSA algorithm, for determining the incoming direction of the γ ray, to be used in the Doppler correction formula (this method was named "PSA+1HitID"). It has to be specified that this in-beam test was

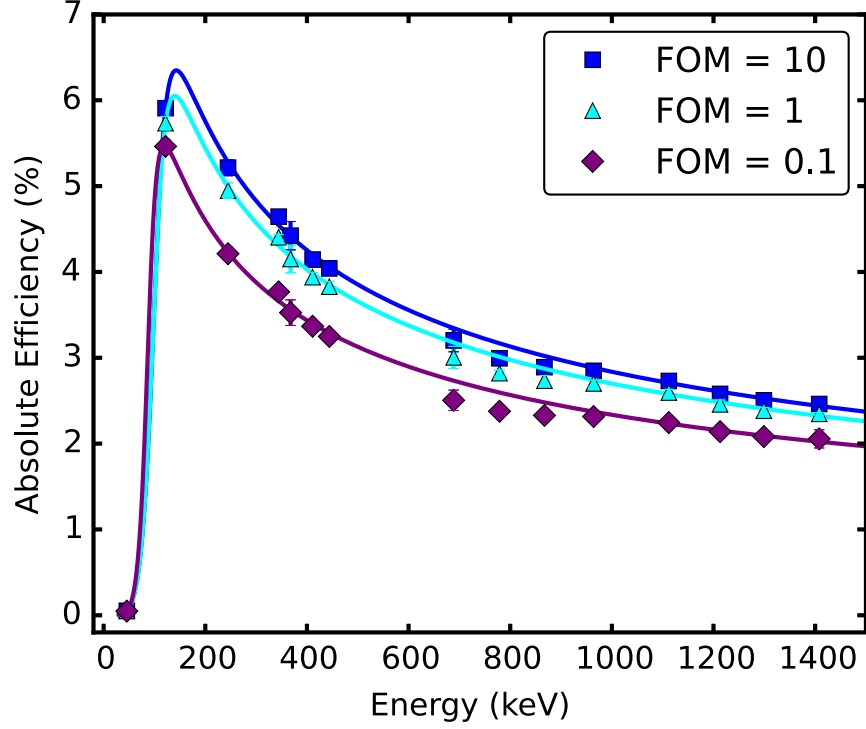
performed at LNL in 2010: only two clusters of AGATA were present during the experiment and significant improvement in the treatment of pair production events in the tracking software was made after that time. Moreover, the fact that the "PSA+1HitID" works better than the standard tracking is strictly connected to the γ multiplicity ($M=1$) situation and the minimal presence of background radiation. In these specific conditions, the presented results might suggest a simple and efficient alternative to standard tracking.

5.4 Performance of γ -ray tracking with AGATA coupled to different detector systems

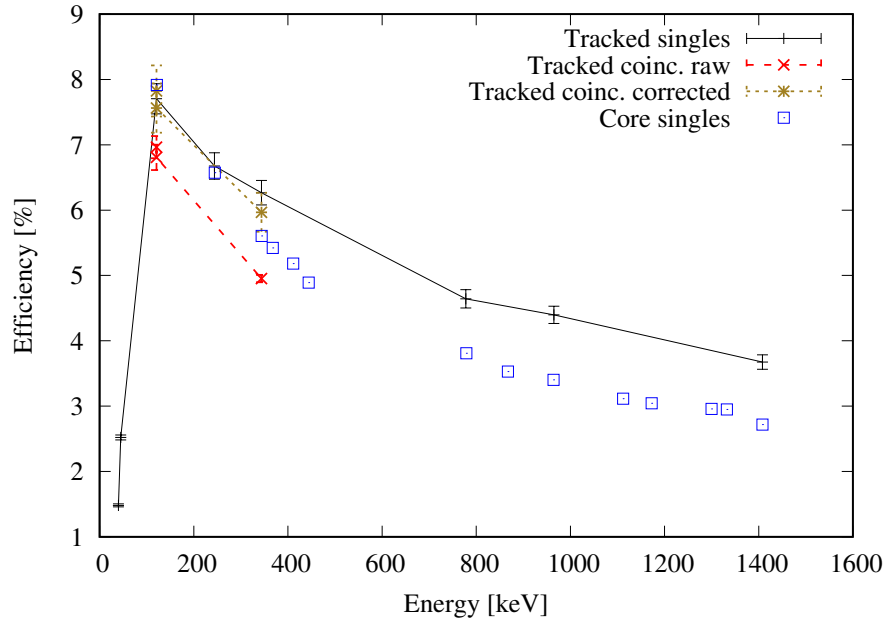
To increase the sensitivity of the experimental setup γ -ray spectrometers are often coupled to other detector systems. Examples are the use of magnetic spectrometers [43, 44] for event-by-event identification of the reaction product. Particle detectors to count charged particles and/or neutrons originating from the reaction are also used to enhance the wanted reaction channel in the γ -ray spectra [45, 46, 47]. The use these ancillary detectors with AGATA is described in previous papers [36, 48, 49] and will not be further discussed here, and we will focus on how different categories of ancillary detectors impact the γ -ray tracking performance.

Large acceptance magnetic spectrometers have an impact on the spectra after γ -ray tracking. As shown in figure 6 a large back-scattering peak is present in the experimental data that is not present in simulated data unless a large block of steel is introduced in the simulation. This block of steel represents the entrance quadrupole magnet of PRISMA [43]. All γ -ray tracking algorithms have problem discriminating against these back scattered γ rays as they come from a direction close to that of the target position. The back scattered γ rays are more present in γ -ray tracking arrays than in arrays using Compton Shields because the γ -ray tracking offers less effective collimation than the Compton Shields.

The use of ancillary particle detectors or other types of devices such as a Plunger that are positioned between the target and AGATA will generate scattering and absorption of the emitted γ rays. However, for situations where AGATA only covers a fraction of the solid angle it is possible to minimise these losses using reasonable designs. Examples of losses in efficiency is given in figure 7 for the case of using the OUPS plunger or the MUGAST[47] detector system. The effect in these cases, with AGATA covering less than 1π of solid angle, is limited to low energies and moderate in magnitude.



(a) Efficiency after γ -ray tracking as a function γ -ray energy for different the Figure-Of-Merit (FOM) used in MGT to decide if a cluster of interaction points is correctly tracked. A FOM=1 is the default used in MGT. Figure taken from Lalović et al. [37]



(b) Efficiency after γ -ray tracking as a function γ -ray energy for singles and coincidence measurements using the OFT code. The efficiency using the sum of crystal (called core singles) is also shown. Figure from Ljungvall et al. [25].

Figure 4: Efficiency after γ -ray tracking for AGATA at GSI (a) and AGATA at GANIL(b), respectively. For GSI the MGT [14] code was used for tracking. The OFT [12] code was used for the GANIL data.

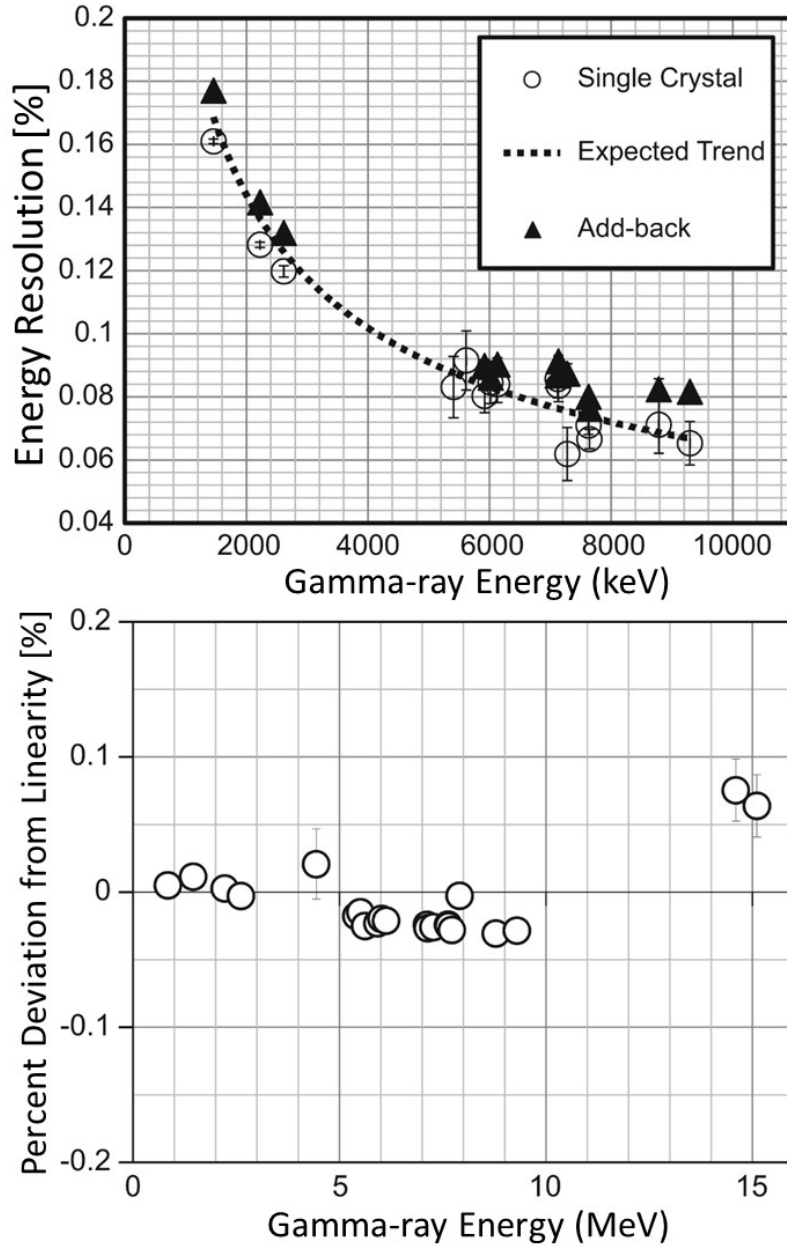


Figure 5: Upper panel: energy resolution of the AGATA detectors up to 9 MeV. The data for the best performing HPGe crystal are shown by empty black circles. The black triangles represent the energy resolution for the add-back procedure (sum of the energies recorded in all the crystals that fired in each event). The experimental data follow the expected $\propto E^{-1/2}$ trend (indicated by the dashed black line). Bottom panel: percent deviation of the measured energies from the tabulated ones, considering a linear calibration. If not displayed, error bars are smaller than the symbol size.

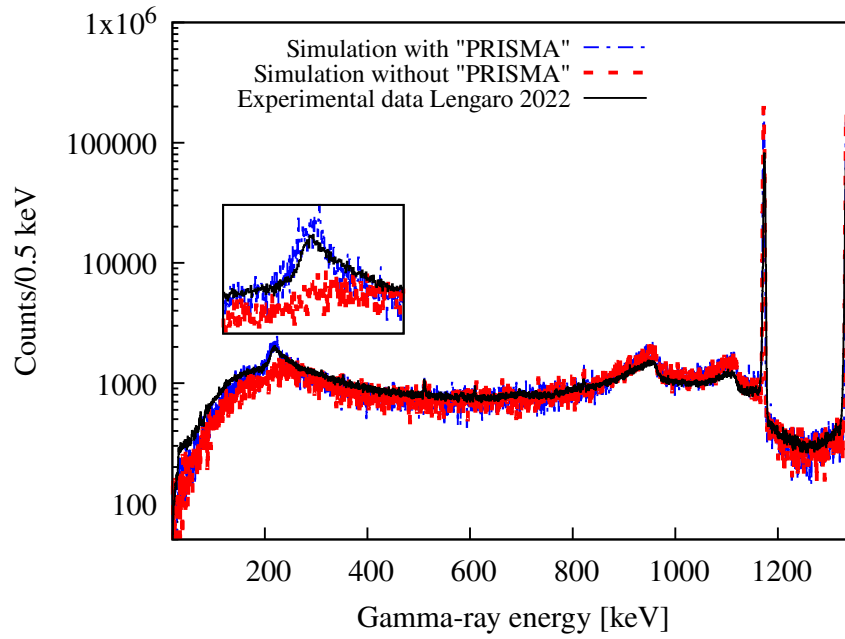


Figure 6: Tracked spectra using a ^{60}Co source. The solid black line is the experimental spectrum, the dashed red line is a simulation without an iron block, and the dashed dotted blue line is the simulation with an iron block modelling PRISMA. The appearance of the back-scattering peak in the simulated data with PRISMA is clear, as shown in the inset. For details see text.

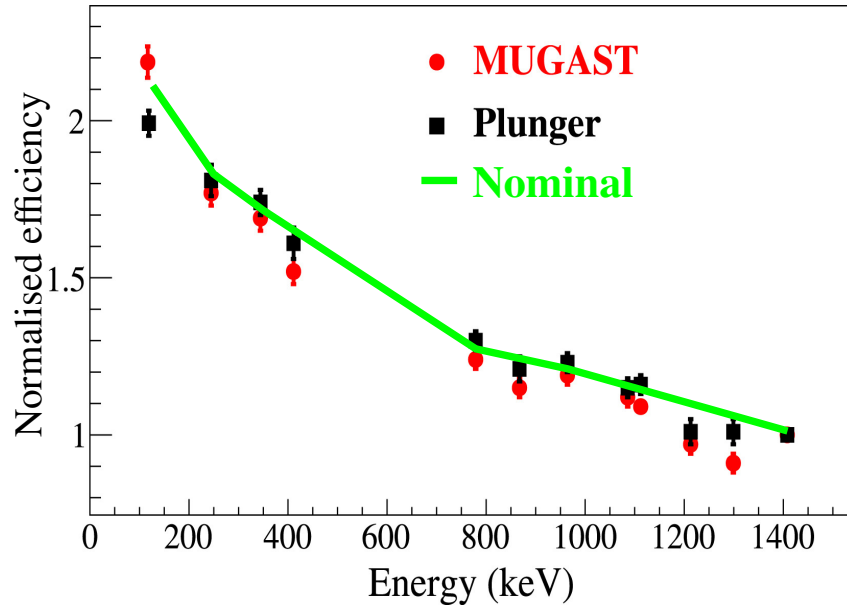


Figure 7: Efficiency, normalised to 1 at 1408 keV, as a function of γ -ray energy. For experimental setups with the OUPS and corresponding chamber, the MUGAST particle detector array, and finally, with only the standard GANIL target chamber. Figure modified from Assié et al. [47] and Ljungvall et al. [25]. For errors on the nominal efficiency see figure 4b.

6 Improvements in γ -ray spectrometer performance due to the γ -ray tracking

In this section we focus on AGATA performances in respect to a few specific aspects, in which the detector millimetric position sensitivity and the tracking technology are of fundamental importance in improving the experimental sensitivity of a high-resolution γ spectrometer.

6.1 Doppler correction

The primary feature of HPGe γ detectors is their excellent energy resolution. For in-beam spectroscopy experiments it can be significantly degraded due to the Doppler effect. This is especially important for experiments done in inverse kinematics, which is often the case for radioactive beam experiments. As Doppler correction is one of the most important gains that PSA and γ -ray tracking offers, we remind the reader that, when the γ rays are emitted in-flight by a recoiling nucleus, the width of peaks in the Doppler-corrected spectra will depend on three factors, namely the intrinsic detector energy resolution, the error on the velocity vector of the emitting nucleus and the uncertainty on the photon direction. The last factor depends on the position resolution of the PSA algorithm used and the capacity of the γ -ray tracking algorithm to correctly determine the first interaction point.

The Doppler-shift formula is the following:

$$E_{\gamma}^{cm} = E_{\gamma} \frac{1 - \beta \cos \theta}{\sqrt{1 - \beta^2}} \quad (5)$$

where E_{γ}^{cm} is the CMS energy of the γ ray, E_{γ} is the energy of the photon in the laboratory (in other words the energy seen by the detector), β is the velocity of the emitting nucleus and θ is the angle between the direction of the recoiling nucleus and the direction of the photon in the laboratory. Each of the parameters entering the formula contributes to the final uncertainty. Quantitatively, the contribution of each parameter to the final position resolution is evaluated through the propagation of errors on E_{γ}^{cm} , giving:

$$\begin{aligned} (\Delta E_{\gamma}^{cm})^2 &= \left(\frac{\partial E_{\gamma}^{cm}}{\partial \theta} \right)^2 (\Delta \theta)^2 + \\ &+ \left(\frac{\partial E_{\gamma}^{cm}}{\partial \beta} \right)^2 (\Delta \beta)^2 + \\ &+ \left(\frac{\partial E_{\gamma}^{cm}}{\partial E_{\gamma}} \right)^2 (\Delta E_{\gamma})^2. \end{aligned} \quad (6)$$

In this calculation, the different broadening sources are considered as statistically independent contributions, neglecting for simplicity any correlation between them. In Eq. 6, $\Delta \beta$ and $\Delta \theta$ are respectively the uncertainty on the

velocity module and on the angle between the direction of the nucleus emitting the radiation and the emitted γ ray. Even if the recoil velocity vector can be measured on an event-by-event basis, $\Delta\beta$ and $\Delta\theta$ will be generally non-zero. The term ΔE_γ in Eq. 6 describes the contribution of the intrinsic energy resolution of the detector.

The partial derivatives are:

$$\begin{aligned}\frac{\partial E_\gamma^{cm}}{\partial \theta} &= E_\gamma \frac{\beta \sin \theta}{\sqrt{1 - \beta^2}} \\ \frac{\partial E_\gamma^{cm}}{\partial \beta} &= E_\gamma \frac{\beta - \cos \theta}{(1 - \beta^2)^{3/2}} \\ \frac{\partial E_\gamma^{cm}}{\partial E_\gamma} &= \frac{1 - \beta \cos \theta}{\sqrt{1 - \beta^2}}\end{aligned}\tag{7}$$

The angular error is propagated to the error in the determination of the CMS energy of the γ ray by the coefficient given in the first row of Eq. 7. As an example, the contributions of the three sources of Doppler broadening are sketched in Fig. 8, for the case of photons of 1 MeV emitted from a nucleus in motion with $\beta = 20\%$ and detected with an uncertainty $\Delta\theta = 1^\circ$ on its direction. It is thanks to PSA and γ -ray tracking that a $\Delta\theta$ as low as 1° is imaginable while still keeping such large γ -ray efficiency.

As just mentioned, the γ -ray tracking technology of AGATA allows reconstructing the emission angle of the γ ray with a precision of about 1 degree and, consequently, to recover a large fraction of the energy resolution degraded by the Doppler broadening. As a visual example, the improvement in the quality of a γ -ray spectrum obtained thanks to γ -ray tracking, can be appreciated by looking at the difference between the grey line spectrum and its fully Doppler corrected version (red line) in Fig. 9.

In order to appreciate in a more quantitative way the improvement in resolution, it is important to consider in some detail the experimental situation in which this spectrum was acquired. The theta angle that appears in the Doppler shift formula is actually the angle between the direction of the γ and the velocity vector of the emitting nucleus. Therefore, also the precision in the experimental determination of the latter quantity is of relevance, in general, for the Doppler correction quality. The 6.13 MeV γ line, showed in the figure, is emitted by the ^{16}O excited nucleus ($3_1^- \rightarrow 0_{g.s.}^+$) moving at a velocity of around the 20% of the speed of light. This nucleus is produced in the reaction ($^{17}\text{O}, ^{16}\text{O}'n\gamma$), induced with a ^{17}O beam at 20 MeV/u impinging on a ^{208}Pb target at LNL lab [51]. This specific reaction channel was selected by detecting the generated ^{16}O nuclei with a segmented Silicon pad detector (TRACE [36, 52]) which allowed, in fact, a precise experimental determination of their velocity vector. This precise measurement of the velocity direction for the γ emitting nucleus was crucial for allowing to maximise the quality of Doppler correction and, also, to obtain γ -ray angular distribution plots that will be shown later.

The increase in resolving power from the combination of PSA and γ -ray tracking for prompt γ -ray spectroscopy is clear when combined with magnetic

spectrometers giving the precise recoil vector of the decaying nucleus. Lemasson et al. (see figure 3 in Lemasson et al. of this issue) give as an example the spectroscopy of ^{98}Zr after the fusion-fission with a ^{238}U beam at 6.2 MeV/A and a ^9Be target. Here the FWHM of the 1229.9 keV γ ray from the $2_1^+ \rightarrow 0_1^+$ transition varies from 15 keV for the EXOGAM array to 5 keV for AGATA while covering similar angular ranges.

The good Doppler correction capability of AGATA makes it a powerful tool for lifetime measurements using Doppler Shift methods such as Recoil-Distance Doppler Shift (RDDS) or Doppler-Shift Attenuation Method (DSAM). Using AGATA it is possible to measure lifetime from a few fs with DSAM, to hundreds of ps with RDDS. Fast timing methods using ancillary detectors can be used to complementary AGATA allowing, with one experiment setup, the measurement of fs to ns. It is therefore not surprising that in all three AGATA campaigns (Legnaro, GSI, and GANIL) lifetime measurements have constituted a significant fraction of the performed experiments. For a multitude of examples see Bracco et al. [7] and Lemasson et al. [53] and Gadea et al. [54] in this issue.

Detailed quantitative investigations have been performed in order to study the impact of the position resolution from PSA in limiting the Doppler correction quality in AGATA ([24, 55]). They all consistently point to a ≈ 5 mm FWHM average position resolution value. This value, however, can change depending on the region of the detector segment in which the interaction took place and, of course, on the amount of energy released in the γ hit.

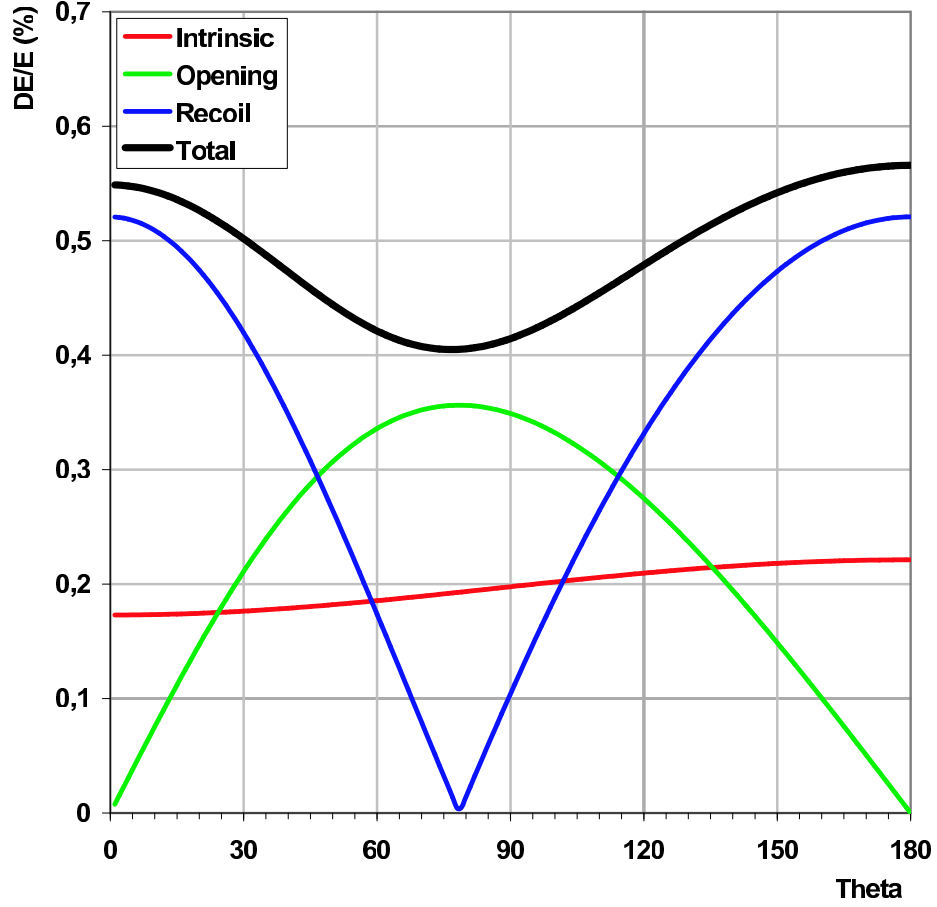


Figure 8: The contributions of the different Doppler broadening sources as a function of the azimuthal angle of the detector with respect to the direction of the recoil emitting the radiation. A photon energy of 1 MeV is assumed, with a typical energy resolution for a germanium detector, producing the “Intrinsic” contribution (in red); a source velocity of $\beta = 20.0\%$ with an error of 0.5%, giving the “Recoil” contribution (in blue); an uncertainty $\Delta\theta = 1^\circ$ in the source direction, obtaining the “Opening” contribution (in green). Taken from [50].

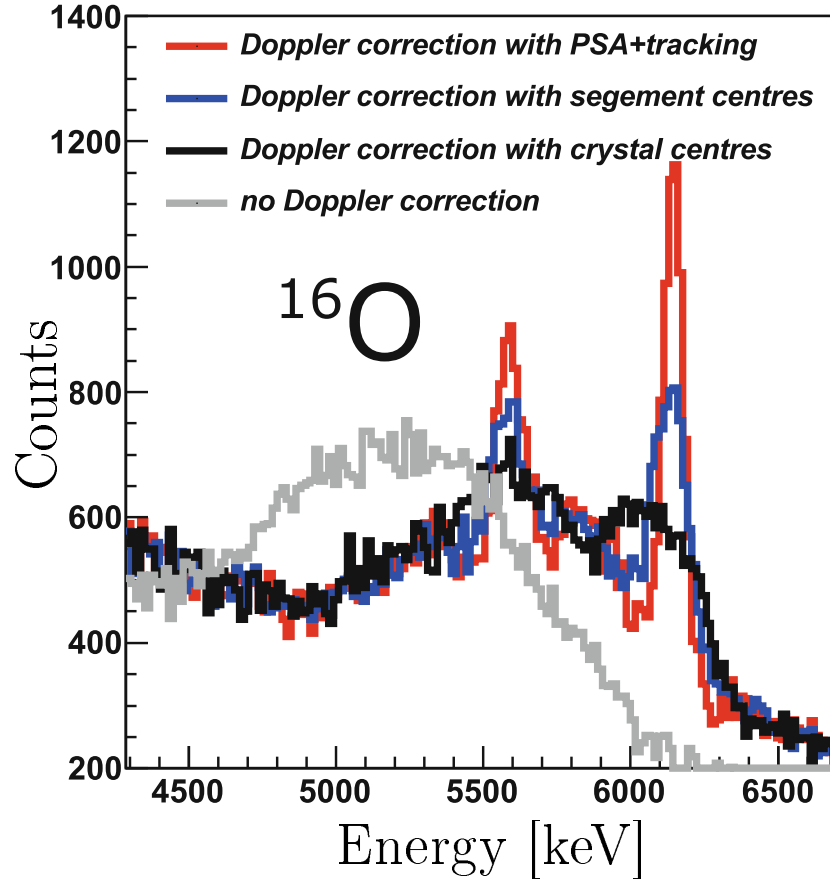


Figure 9: Energy spectrum of the γ rays measured in correspondence of the $(^{17}\text{O}, ^{16}\text{O}'\text{n}\gamma)$ reaction channel [51]. The grey spectrum is without Doppler correction, while the others were corrected using position information at different precision level, as described in the legend. The case of a standard HPGe detector (i.e. with no position sensitivity) corresponds to the black line histogram.

6.2 Background suppression

In AGATA, the Compton background suppression is performed via γ -ray tracking (thus eliminating the necessity of using BGO shields). The goodness of the suppression is quantified using the peak to total ratio. The most recent work studying this parameter for AGATA is [25]. It was determined for ^{60}Co source data and compared with simulations. The peak-to-total value for the 1173 keV peak of ^{60}Co was measured to be 36.4(4)%. The background is mainly due to single-interaction points considered, erroneously, by the tracking as full-energy-peak events. Excluding such events the peak-to-total is increased to 52.4(6)%, but with a reduction in efficiency of 17%. In fact, the more stringent values of tracking algorithm parameters we set, the cleaner spectra we obtain. It is good practice to optimise the γ -ray tracking parameters for each experiment as the optimal values are γ -ray energy and multiplicity dependant.

Another kind of background that is commonly present in the experiments is the one originating from neutrons. The possibility to suppress this background is discussed in section 6.4 of this manuscript. Finally, since a properly tracked, and accepted, γ ray should always originate from the target position, the background γ rays originating from locations that are far from the target position should be significantly reduced in the spectra. Different techniques to achieve this are discussed in section 7 as they fall under γ -ray imaging techniques. This is particularly relevant for experiments with relativistic exotic beams at GSI. In setups as RISING [56], in fact, sources of significant background radiation were found to be materials of different origin placed around the target (e.g. other detectors, degraders, the target structure itself).

6.3 Angular distributions and Polarisation

The millimetric spatial sensitivity of AGATA detectors allows measuring in a quasi-continuous way the emission direction of a γ ray emitted from the target position. AGATA is hence well suited for measurements of angular distributions, angular correlations, and γ -ray polarisation. In many in-beam nuclear reactions the generated degree of spin alignment allows observing the angular distribution of γ rays emitted following the de-excitation of a nucleus. This allows to study the characteristic angular dependence due to the multipolarity of the emitted γ rays. In Fig. 10 angular distributions measured with AGATA are displayed. These results were extracted with the experimental setup described in [51]. The angle associated to the x-axis of the plots is the angle between the emitted γ ray and the velocity vector of the de-exciting recoiling nucleus (see discussion of inelastic scattering reactions in e.g. [57, 58]). Measuring precisely the direction of the recoiling nucleus, as was done in the experiment of Bracco et al. [51], increases the alignment of the reaction and gives very pronounced angular correlations. In the case of the decay of nuclei that lack spin alignment or polarisation, information on the multipolarity of the electromagnetic nuclear decays can be extracted performing angular correlation measurements between two γ -rays emitted in cascade. The use of AGATA for these kind of

measurements was investigated in [25] using source data.

From a physicist's point of view, it is appealing to have a device capable of measuring with improved sensitivity the polarisation of electromagnetic radiation. In AGATA, this is achieved thanks to the PSA and tracking, providing an improved precision measurement of the azimuthal angle in the Compton scattering process (i.e. quasi-continuous angle Compton polarimetry [59]). Regarding in-beam γ spectroscopy for nuclear structure studies, polarisation measurements are typically used for the determination of the parity of nuclear excited states. Technical works were dedicated to the investigation of the ability of AGATA detectors to measure the polarisation of γ rays [60, 61]. Finally, it is worth to mention that an additional technique, based on a different principle than the quasi-continuous angle Compton polarimetry (named Coulex-multipolarimetry with relativistic heavy-ion beams), but still taking advantage of the position sensitivity of the detectors, has been developed and bench-marked [62, 63].

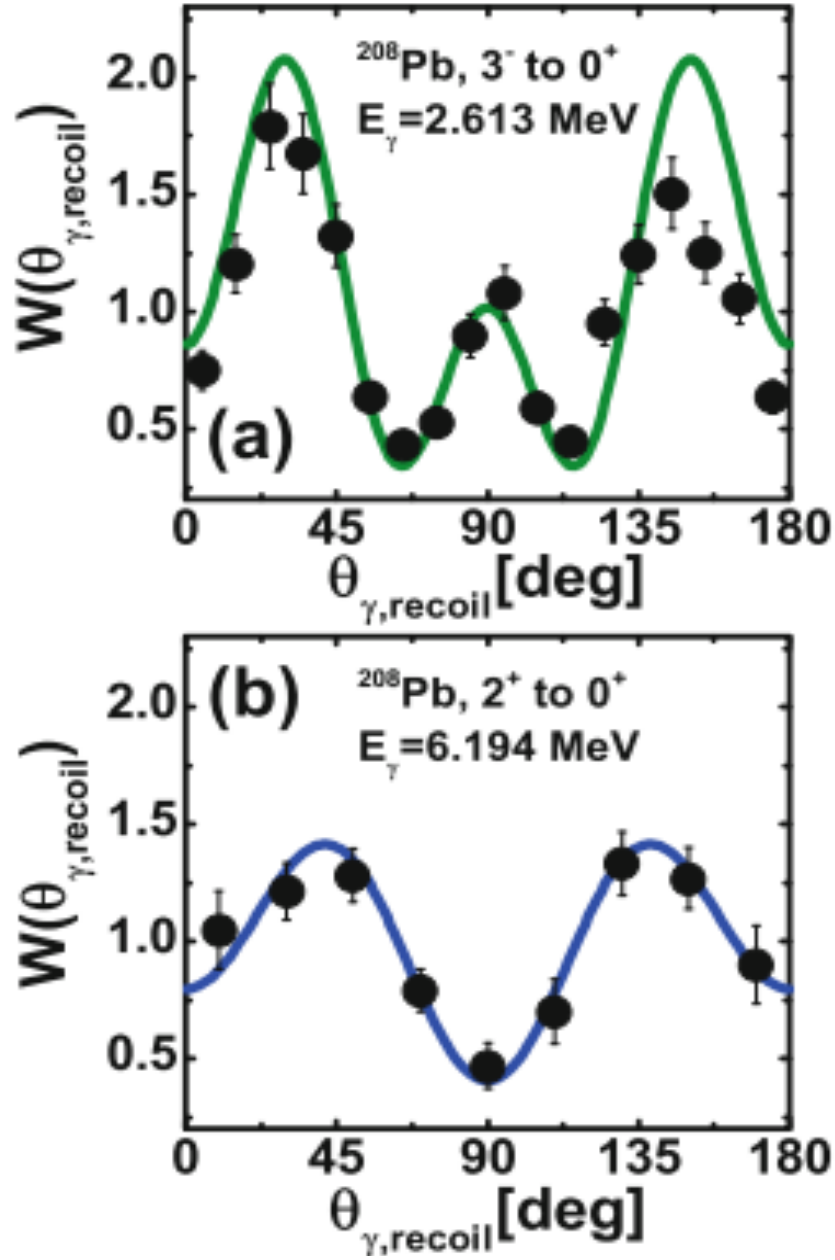


Figure 10: Distribution plots showing the angular correlation $\theta_{\gamma, \text{recoil}}$ (between the emitted γ rays and velocity vector of the de-exciting recoiling nuclei), for two different transitions of ^{208}Pb , each one having a distinct multipole character (octupole, quadrupole). Looking to Figure 10 in reference [51] it can be appreciated how the angle between the vector associated to the γ direction (included in the solid angle covered by the 5 ATCs²⁶) and the vector associated to the recoil direction (calculated on the basis of the ^{17}O angles covered by the solid angle of TRACE) spans from 0 to 180 deg. The figure is adapted from reference [51].

6.4 Neutron- γ discrimination

It was early on recognised in the AGATA project that a 4π HPGe detector array would detect neutrons emitted in nuclear reaction with high efficiency. This can be viewed either as a problem - the neutrons detected in AGATA generate background in the γ -ray spectra, or as a possibility to use AGATA as a neutron multiplicity filter. Neutron induced background is not something unique to AGATA, and “neutron bumps” associated with in-elastic scattering of neutrons on germanium are a common feature in the γ -ray spectra for Compton-suppressed spectrometers such as EUROBALL [64] as well. The difference with a γ -ray tracking array such as AGATA is the larger solid-angle and that the γ -ray tracking concept mixes energy depositions from different detectors. This later aspect means that a neutron interacting in one detector element can interfere with γ rays detected in adjacent detector elements.

Motivated by both the possibilities and potential issues with neutrons in AGATA a set of investigations have been performed. The study by Ljungvall et al. [65] sought to find pulse-shape differences for signals originating from scattering neutrons or γ rays. Two different N-type HPGe detectors, one of closed-ended coaxial geometry and one of planar geometry, were irradiated with neutrons and γ rays from a ^{252}Cf source. No significant difference between signals originating from scattered neutrons or γ rays was found. As the possibility to separate interactions from neutrons and γ rays based on the pulse shapes is small, other methods have been developed. They aim more at reducing the background generated by $(n, n'\gamma)$ reactions on the Ge isotopes in the detectors rather than using AGATA as a neutron multiplicity filter. In the work by Ljungvall et al. [66] Geant4 Monte-Carlo simulations using the AGATA code [6] were made for different neutron and γ ray distributions. The simulations show a detection efficiency for neutrons from typical nuclear reactions of about 40% for AGATA. Furthermore, it was shown that counting the number of neutrons that interacted in AGATA is challenging. AGATA can hence not be used as a neutron multiplicity filter. This is easily understood, as the majority of neutrons are detected by the γ ray emitted in the inelastic scattering process. Spatial and energy distributions of the interaction of neutrons and γ rays were also compared. The impact on γ -ray tracking performance was studied and quantified using two metrics, Photo-peak efficiency ϵ_{ph} , and for the Peak-To-Background (PTB) defined as the area of the γ -ray peak and the area of the background in a region $\pm\sigma$ around the centroid of the γ -ray peak. The authors used a combination of forward tracking (OFT) and back tracking [12]. The authors concluded that neutrons that scatter inside AGATA do reduce the efficiency and PTB. However, they also pointed out that for traditional γ -ray spectrometers this effect is at least as large and hence not a problem that is aggravated by γ -ray tracking. This was an important result. It should be noted that thanks to PSA it is possible to correct for hole trapping coming from crystal damage from the fast neutrons. For details see Boston et al. [67] in this issue and references therein. Ljungvall et al. [66] also investigated three different parameters to separate neutrons and γ rays from neutron interaction from γ rays originating

at the target positions:

1. Time of Flight. For the nominal distance between AGATA and the target of 25 cm, the time resolution of the large volume HPGe crystals used in AGATA is however not sufficiently high.
2. $\Delta(\cos\theta)$, refers to the use of equation 3 in figure 1 for the first vertex in a track. This is of course at the heart of γ -ray tracking, but here the supplementary condition was only applied to the first vertex.
3. Ratio of low-energy interactions, defined as the number of interaction points with an energy below 20 keV to the total number of interaction points.

The performance of the suggested methods were evaluated for ϵ_{ph} PTB, and the $\Delta(\cos\theta)$ gives an improved PTB of a factor of 3 with a loss in ϵ_{ph} of about 30%.

A similar investigation, but using the MGT tracking code[28], was performed by Ata et al. [68]. In addition to the condition on the difference between the scattering angle of the first vertex calculated using the interaction positions or the deposited energies they also investigated the effects of gates on the energy of the first and second interaction point in accepted tracks, and the use of a gate on the acceptance limit. One can note that Ata et al. used a condition on the angle and not the cosine of the angle, as was the case for Ljungvall et al. There is also a noticeable difference in how the $\Delta(\theta)$ (or $\Delta(\cos\theta)$) condition is used. Ata et al. only applied it to clusters with more than 2 interaction points as simulations had shown that accepted clusters originating from neutron-induced γ rays on average have one interaction point more. The results show an improvement over the work of Ljungvall et al. [66], with a smaller loss in Photo-peak efficiency.

The discrimination methods developed by Ata et al. [68] have also been applied to experimental data from the demonstrator phase of AGATA. enyiğit et al. [69] report on an experiment in which 4 AGATA triple clusters were mounted together with 16 BaF₂ detectors from the HELENA detector array. A ²⁵²Cf source was positioned close to the BaF₂ detectors and 50 cm from the AGATA detectors. The large distance between the ²⁵²Cf source and the AGATA detectors allowed for a discrimination between neutron-induced interactions and γ -ray induced interactions using Time Of Flight. In figure 11 γ ray spectra from neutron induced reactions in the AGATA detectors are displayed. Shown are the sum of core signals (in black), the result of γ -ray tracking (in blue), and tracked with conditions applied to discriminate against neutron-induced γ rays (in red). See the work of enyiğit et al. [69] for details. Already γ -ray tracking discriminates well against neutron-induced γ rays, as the blue spectrum contains much less intensity in the (n,n' γ) lines than the black spectrum. An example of such a transition is marked with an ellipse in figure 11. This discrimination is easy to understand as the γ rays from (n,n' γ) do not originate from the assumed target position. By applying gates on tracking parameters, see enyiğit et al. [69] a further reduction of neutron-induced γ rays is seen. The reduction of counts

in the γ -ray spectra coming from $(n,n'\gamma)$ is about 40% (red spectrum). Source data using ^{60}Co showed a loss of efficiency close to 20% for γ rays originating from the target position.

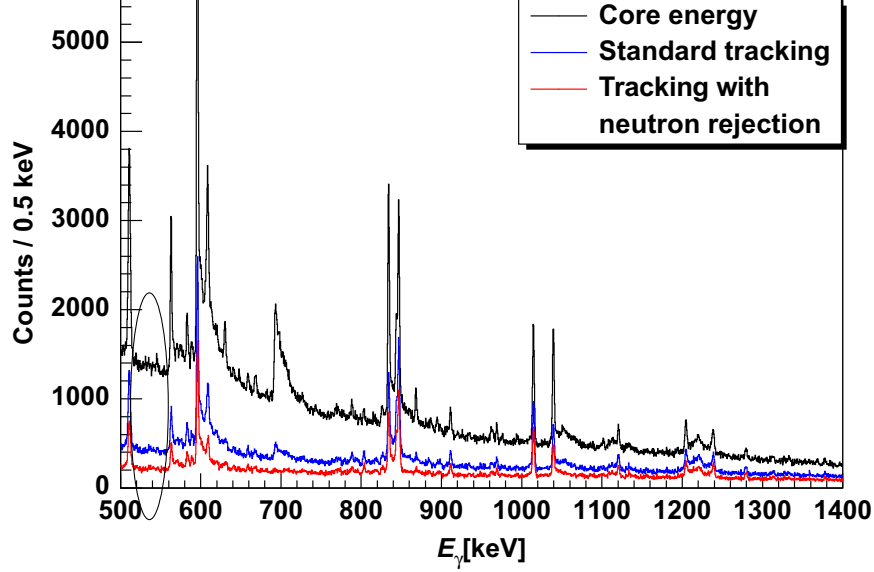


Figure 11: Gamma-ray spectra showing the energy deposition in AGATA when irradiated with neutrons from a ^{252}Cf source. The black spectrum corresponds to the sum of the core signals and shows clear neutron-induced γ rays with corresponding triangular shapes. The blue line is after γ -ray tracking showing that already the standard γ -ray tracking discriminates well against neutron-induced interactions. The red spectrum is after having applied the additional gates used to suppress the neutron-induced interaction. An ellipse highlights the γ transition $2_1^+ \rightarrow 0_1^+$ in ^{74}Ge excited by $(n,n'\gamma)$ reactions. This figure is modified from Şenyiğit et al. [69].

It has been proposed to look for isolated hits with an energy of about 690 keV, corresponding to the E0 transition in ^{72}Ge , combined with PSA as a method to counts neutrons with an efficiency of about 1.5% [70]. It is a too low efficiency to be of interest for nuclear structure experiments, and is too specialised for discrimination of the γ ray background generated by the fast neutrons.

As a concluding remark on the work done to discriminate between neutron-s/neutron induced γ rays and γ rays one can state that the developed methods do not allow the use AGATA as a neutron multiplicity filter nor to completely remove the background induced by neutrons. Their use on experimental data has, to our knowledge, up to now been very limited.

7 Gamma-ray imaging techniques and γ -ray tracking

Early in the development of γ -ray tracking the connection with γ -ray imaging was made: the ordering of the γ -ray interaction allows the reconstruction of a cone of origin for the γ ray. This is illustrated in figure 12. An example of early exploratory work (within what was to become the AGATA community) is that of van der Marel et. [71]. The back tracking algorithm was used to assess the performance of a setup consisting of two (hypothetical) planer HPGe detectors. Rather promising results are shown for SPECT and PET applications, although it should be mentioned that very optimistic assumptions on the achievable position resolution were made. Another study of possible applications using γ -ray tracking, and this time with AGATA crystals, is that of Gerl [72]. It is stated that the experimentally achieved position ($\sigma = 2mm$) and energy (2.1keV@1.3MeV FWHM) resolution is adequate for both nuclear safety and medical applications.

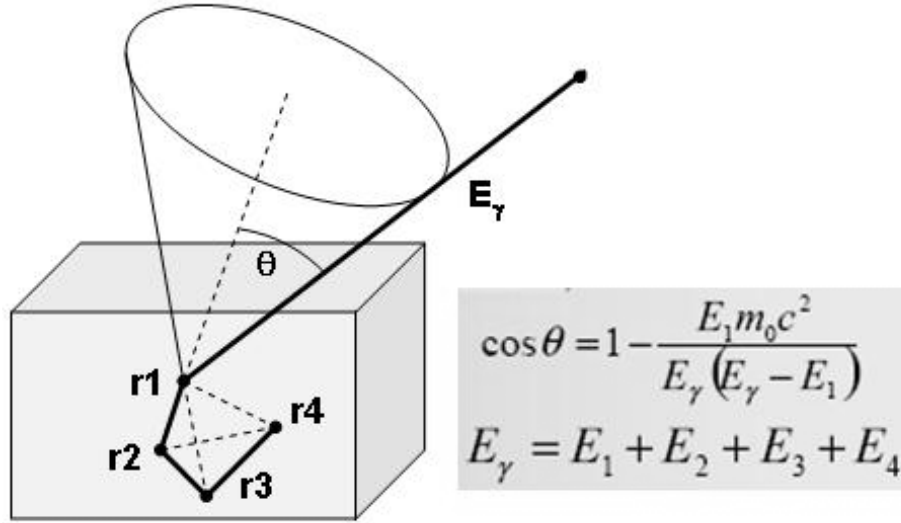


Figure 12: Figure showing the principle of γ ray imaging using γ -ray tracking. The crossing of many cones builds up the image. Figure from J. Gerl [72].

Multiple investigations have also been made using AGATA detectors combined with other detectors in order to improve the Compton imaging performance [73, 74]. These investigations are not in the scope of this article.

Compton imaging has also been used to characterise the performance of AGATA [23] and to improve the background rejection using imaging techniques [75]. In the work of Recchia et al.[23] Compton imaging is used to estimate the position resolution achieved by the PSA algorithms in AGATA. In

the paper the different contributions to the angular resolution of “cones” (see figure 12) given by the Compton formula are calculated. It is shown that the angular resolution is dominated by the incertitude coming from the PSA determining the position of the γ -ray interaction. Imaging can therefore estimate the achieved position resolution. The method to estimate the position resolution used by Recchia et al. is to compare images reconstructed using experimental data and images reconstructed using simulations, in which the assumed position resolution is varied. A ^{60}Co source was placed 1 m from the AGATA detector. After PSA and a simplified γ -ray tracking, consisting in assuming that the interaction point with the largest deposited energy is the first, the so-called back-projection method [76] was used to create the images. By comparing the FWHM of the projection on one axis of the image the position resolution is deduced. The result is compatible with in-beam measurements using the Doppler shift to deduce the PSA resolution [24].

Another example of the connection between Compton imaging γ -ray tracking is the use of imaging to suppress background in γ ray spectra. Doncel et al. [75] used one AGATA detector to quantify how well γ -ray tracking can separate the origin of γ rays. The setup consisted of the AGATA detector surrounded by three γ -ray source, ^{60}Co , ^{137}Cs , and ^{152}Eu . Using a simplified tracking al-

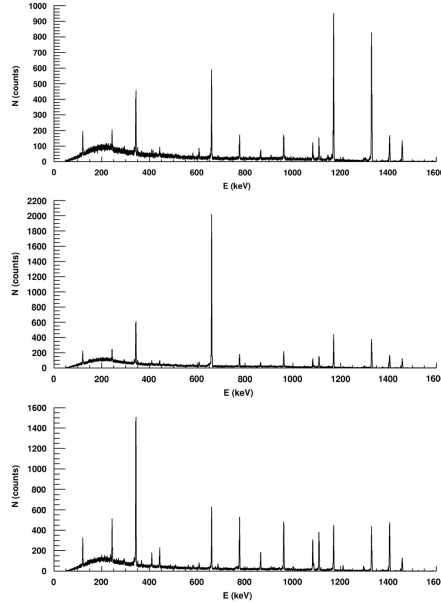


Figure 13: Spectrum from ^{60}Co incremented when the difference for $\theta_C - \theta_G$ was smallest for the position where the from ^{60}Co source was located (top panel). Middle and bottom panel show the same thing but for ^{137}Cs and ^{152}Eu , respectively. Figure from Doncel et al.[75].

gorithm adapted to experimental setup consisting of one symmetric AGATA crystal it was shown that comparing the scattering angle as given by the energy deposition with the angle coming from geometrical considerations a suppression of background from γ -ray sources of known origin with a factor of 3 is possible. In figure 13 spectra incremented based on the difference between the first scattering angle as calculated by the first energy deposition θ_C and the angle given by the source position, the first, and second interaction points, called θ_G . A clear enhancement for the γ ray originating from the correct source can be seen. This method is of interest to identify unknown γ rays in spectra by creating spectra assuming different origin of the γ rays when doing the γ -ray tracking. To our knowledge this has however not been exploited when performing γ -ray tracking.

8 Conclusions and Perspective

Over the last 15 years γ -ray tracking has proved itself as a viable way of constructing high-performance high-resolution γ -ray spectrometers using HPGe detectors. Developed using Geant4 simulations of ideal 4π spheres the algorithms have been adapted to experimental data and the defaults of PSA and provide performance close to what was projected based on the simulations. The ability to identify the first interaction point of a γ ray with a precision of less than 5 mm is a huge advantage for in-beam γ -ray spectroscopy allowing to recover the intrinsic high energy resolution of the HPGe detectors. It also allows for high precision lifetime measurements using Doppler Shift methods with an unprecedented sensitivity.

As this review is written it is believed, but not proven, that improving the γ -ray tracking algorithms presently used by the AGATA and GRETA collaborations requires event-by-event errors on position (and energy partitioning in the case of multiple hits in an segment) coming from the PSA. A better estimation of the number of scatterings a γ ray really underwent before absorption is also welcome. A tracking algorithm that possesses such complete information will provide better discrimination between fully absorbed γ rays and γ rays that scattered out of the array.

A closer coupling between PSA and γ -ray tracking is also envisioned. This can be either by a PSA providing multiple solution to γ -ray tracking, and hence relying on γ -ray tracking to solve the problem of identifying the correct number of interactions a γ ray has undergone before absorption. Here the general structure of the Data Acquisition system dividing AGATA into local (detectors and hence PSA) and global levels (e.g. tracking) can be kept. However, the combinatorial nature of the problem might lead to computational challenges. An even more ambitious idea is to combine PSA and γ -ray tracking in one large minimisation process. It would not only require an important computational effort but also exploratory work investigating how to combine the figure-of-merits of PSA and γ -ray tracking.

The use of machine learning for γ -ray tracking has already started and at the

time of writing this paper (2022) it seems to be a promising avenue to follow.

The authors would like to thank the AGATA collaboration. The AGATA project is supported in France by the CNRS. Data used for this publication were collected at INFN Legnaro, GSI, and GANIL and this work would not have been possible without the valuable contributions from these laboratories and their staff.

References

- [1] S. Akkoyun et al., Agata-advanced {GAMMA} tracking array, Nuclear Instruments and Methods in Physics Research Section A: Accelerators, Spectrometers, Detectors and Associated Equipment 668 (2012) 26 – 58.
doi:<http://dx.doi.org/10.1016/j.nima.2011.11.081>.
URL <http://www.sciencedirect.com/science/article/pii/S0168900211021516>
- [2] I.Y. Lee, Gamma-ray tracking detectors, Nuclear Instruments and Methods in Physics Research Section A: Accelerators, Spectrometers, Detectors and Associated Equipment 422 (1) (1999) 195–200.
doi:[https://doi.org/10.1016/S0168-9002\(98\)01093-6](https://doi.org/10.1016/S0168-9002(98)01093-6).
URL <https://www.sciencedirect.com/science/article/pii/S0168900298010936>
- [3] I.Y. Lee et al., Gretina: A gamma ray energy tracking array, Nuclear Physics A 746 (2004) 255–259, proceedings of the Sixth International Conference on Radioactive Nuclear Beams (RNB6).
doi:<https://doi.org/10.1016/j.nuclphysa.2004.09.038>.
URL <https://www.sciencedirect.com/science/article/pii/S0375947404009637>
- [4] I Y Lee, M A Deleplanque and K Vetter, Developments in large gamma-ray detector arrays, Reports on Progress in Physics 66 (7) (2003) 1095–1144.
doi:[10.1088/0034-4885/66/7/201](https://doi.org/10.1088/0034-4885/66/7/201).
URL <https://doi.org/10.1088/0034-4885/66/7/201>
- [5] J. Eberth and J. Simpson, From ge(li) detectors to gamma-ray tracking arrays—50 years of gamma spectroscopy with germanium detectors, Progress in Particle and Nuclear Physics 60 (2) (2008) 283–337.
doi:<https://doi.org/10.1016/j.pnpnp.2007.09.001>.
URL <https://www.sciencedirect.com/science/article/pii/S0146641007000828>
- [6] E. Farnea, F. Recchia, D. Bazzacco, Th. Kröll, Zs. Podolyák, B. Quintana and A. Gadea, Conceptual design and monte carlo simulations of the {AGATA} array, Nuclear Instruments and Methods in Physics Research Section A: Accelerators, Spectrometers, Detectors and Associated Equipment 621 (1-3) (2010) 331 – 343.

doi:<http://dx.doi.org/10.1016/j.nima.2010.04.043>.
 URL <http://www.sciencedirect.com/science/article/pii/S0168900210008922>

- [7] A. Bracco, G. Duchêne, Zs. Podolyák and P. Reiter, Gamma spectroscopy with agata in its first phases: New insights in nuclear excitations along the nuclear chart, *Progress in Particle and Nuclear Physics* 121 (2021) 103887. doi:<https://doi.org/10.1016/j.pnpnp.2021.103887>.
 URL <https://www.sciencedirect.com/science/article/pii/S0146641021000417>
- [8] W. Korten et al., Physics opportunities with the advanced gamma tracking array: Agata, *The European physical journal. A, Hadrons and nuclei* 56 (5).
- [9] S. Tashenov and J. Gerl, Tango—new tracking algorithm for gamma-rays, *Nuclear Instruments and Methods in Physics Research Section A: Accelerators, Spectrometers, Detectors and Associated Equipment* 622 (3) (2010) 592–601. doi:<https://doi.org/10.1016/j.nima.2010.07.040>.
 URL <https://www.sciencedirect.com/science/article/pii/S0168900210016505>
- [10] G.J. Schmid et al., A γ -ray tracking algorithm for the {GRETA} spectrometer, *Nuclear Instruments and Methods in Physics Research Section A: Accelerators, Spectrometers, Detectors and Associated Equipment* 430 (1) (1999) 69 – 83. doi:[http://dx.doi.org/10.1016/S0168-9002\(99\)00188-6](http://dx.doi.org/10.1016/S0168-9002(99)00188-6).
 URL <http://www.sciencedirect.com/science/article/pii/S0168900299001886>
- [11] J van der Marel and B Cederwall, Backtracking as a way to reconstruct compton scattered γ -rays, *Nuclear Instruments and Methods in Physics Research Section A: Accelerators, Spectrometers, Detectors and Associated Equipment* 437 (2-3) (1999) 538 – 551. doi:[http://dx.doi.org/10.1016/S0168-9002\(99\)00801-3](http://dx.doi.org/10.1016/S0168-9002(99)00801-3).
 URL <http://www.sciencedirect.com/science/article/pii/S0168900299008013>
- [12] A. Lopez-Martens, K. Hauschild, A. Korichi, J. Roccoz and J-P. Thibaud, γ -ray tracking algorithms: a comparison, *Nuclear Instruments and Methods in Physics Research Section A: Accelerators, Spectrometers, Detectors and Associated Equipment* 533 (3) (2004) 454 – 466. doi:<http://dx.doi.org/10.1016/j.nima.2004.06.154>.
 URL <http://www.sciencedirect.com/science/article/pii/S0168900204014779>
- [13] S. Paschalis et al., The performance of the gamma-ray energy tracking in-beam nuclear array gretina, *Nuclear Instruments and Methods in Physics Research Section A: Accelerators, Spectrometers, Detectors and Associated Equipment* 709 (2013) 44 – 55.

- doi:<https://doi.org/10.1016/j.nima.2013.01.009>.
 URL <http://www.sciencedirect.com/science/article/pii/S0168900213000508>
- [14] Dino Bazzacco, The advanced gamma ray tracking array agata, Nuclear Physics A 746 (2004) 248–254, proceedings of the Sixth International Conference on Radioactive Nuclear Beams (RNB6). doi:<https://doi.org/10.1016/j.nuclphysa.2004.09.148>.
 URL <https://www.sciencedirect.com/science/article/pii/S0375947404009625>
- [15] T. Lauritsen et al., Characterization of a gamma-ray tracking array: A comparison of gretina and gammasphere using a ^{60}Co source, Nuclear Instruments and Methods in Physics Research Section A: Accelerators, Spectrometers, Detectors and Associated Equipment 836 (2016) 46 – 56. doi:<https://doi.org/10.1016/j.nima.2016.07.027>.
 URL <http://www.sciencedirect.com/science/article/pii/S0168900216307434>
- [16] A. Korichi and T. Lauritsen, Tracking γ rays in highly segmented hpge detectors: A review of agata and gretina, The European Physical Journal A 55 (7) (2019) 121. doi:[10.1140/epja/i2019-12787-1](https://doi.org/10.1140/epja/i2019-12787-1).
 URL <https://doi.org/10.1140/epja/i2019-12787-1>
- [17] G. Suliman and D. Bucurescu, Fuzzy clustering algorithm for gamma ray tracking in segmented detectors, Romanian Reports in Physics 62 (1) (2010) 27–36.
- [18] F. Didierjean, G. Duchêne and A. Lopez-Martens, The deterministic annealing filter: A new clustering method for γ -ray tracking algorithms, Nuclear Instruments and Methods in Physics Research Section A: Accelerators, Spectrometers, Detectors and Associated Equipment 615 (2) (2010) 188–200. doi:<https://doi.org/10.1016/j.nima.2010.01.030>.
 URL <https://www.sciencedirect.com/science/article/pii/S0168900210000987>
- [19] D. Bazzacco R. Venturelli, Adaptive grid search as pulse shape analysis algorithm for γ -tracking and results, Tech. rep., LNL (2004).
- [20] S. Agostinelli et al., Geant4—a simulation toolkit, Nuclear Instruments and Methods in Physics Research Section A: Accelerators, Spectrometers, Detectors and Associated Equipment 506 (3) (2003) 250 – 303. doi:[https://doi.org/10.1016/S0168-9002\(03\)01368-8](https://doi.org/10.1016/S0168-9002(03)01368-8).
 URL <http://www.sciencedirect.com/science/article/pii/S0168900203013688>
- [21] L Milechina and B Cederwall, Improvements in γ -ray reconstruction with positive sensitive ge detectors using the backtracking method, Nuclear Instruments and Methods in Physics Research Section A: Accelerators,

- Spectrometers, Detectors and Associated Equipment 508 (3) (2003) 394–403. doi:[https://doi.org/10.1016/S0168-9002\(03\)01698-X](https://doi.org/10.1016/S0168-9002(03)01698-X).
URL <https://www.sciencedirect.com/science/article/pii/S016890020301698X>
- [22] K. Vetter et al., Three-dimensional position sensitivity in two-dimensionally segmented hp-ge detectors, Nuclear Instruments and Methods in Physics Research Section A: Accelerators, Spectrometers, Detectors and Associated Equipment 452 (1) (2000) 223–238. doi:[https://doi.org/10.1016/S0168-9002\(00\)00430-7](https://doi.org/10.1016/S0168-9002(00)00430-7).
URL <https://www.sciencedirect.com/science/article/pii/S0168900200004307>
- [23] F. Recchia, D. Bazzacco, E. Farnea, R. Venturelli, S. Aydin, G. Suliman and C.A. Ur, Performance of an agata prototype detector estimated by compton-imaging techniques, Nuclear Instruments and Methods in Physics Research Section A: Accelerators, Spectrometers, Detectors and Associated Equipment 604 (1) (2009) 60 – 63, pSD8. doi:<https://doi.org/10.1016/j.nima.2009.01.079>.
URL <http://www.sciencedirect.com/science/article/pii/S0168900209001168>
- [24] P.-A. Söderström et al., Interaction position resolution simulations and in-beam measurements of the {AGATA} {HPGe} detectors, Nuclear Instruments and Methods in Physics Research Section A: Accelerators, Spectrometers, Detectors and Associated Equipment 638 (1) (2011) 96 – 109. doi:<http://dx.doi.org/10.1016/j.nima.2011.02.089>.
URL <http://www.sciencedirect.com/science/article/pii/S016890021100489X>
- [25] J. Ljungvall et al., Performance of the advanced gamma tracking array at ganil, Nuclear Instruments and Methods in Physics Research Section A: Accelerators, Spectrometers, Detectors and Associated Equipment 955 (2020) 163297. doi:<https://doi.org/10.1016/j.nima.2019.163297>.
URL <http://www.sciencedirect.com/science/article/pii/S0168900219315475>
- [26] N.J. Hammond, T. Duguet and C.J. Lister, Ambiguity in gamma-ray tracking of ‘two-interaction’ events, Nuclear Instruments and Methods in Physics Research Section A: Accelerators, Spectrometers, Detectors and Associated Equipment 547 (2) (2005) 535–540. doi:<https://doi.org/10.1016/j.nima.2005.03.148>.
URL <https://www.sciencedirect.com/science/article/pii/S0168900205009071>
- [27] M. Labiche et al., Simulation of the agata array and coupling with ancillary detectors, EPJ A.

- [28] D. Bazzacco, mgt code developed within the tmr program ‘gamma-ray tracking detectors’.
- [29] Th Kröll et al., Gamma-ray tracking with the mars detector, The European Physical Journal A - Hadrons and Nuclei 20 (1) (2003) 205–206. doi: 10.1140/epja/i2002-10355-6.
URL <https://doi.org/10.1140/epja/i2002-10355-6>
- [30] A. Korichi and T. Lauritsen, In preparation.
- [31] A. Lopez-Martens, AGATA tracking code improvement, Second AGATA-GRETINA Collaboration meeting, (2018).
URL <https://indico.in2p3.fr/event/16944>
- [32] Philipp Napiralla, Employing γ -ray tracking as an event-discrimination technique for γ -spectroscopy with agata, Phd thesis, Technische Universität Darmstadt, Darmstadt, Germany, date Deposited: 2019-12-17 (12 2019).
URL <http://nbn-resolving.de/urn:nbn:de:tuda-tuprints-96737>
- [33] P. Napiralla et al., Approach to a self-calibrating experimental γ -ray tracking algorithm, Nuclear Instruments and Methods in Physics Research Section A: Accelerators, Spectrometers, Detectors and Associated Equipment 955 (2020) 163337. doi:<https://doi.org/10.1016/j.nima.2019.163337>.
URL <http://www.sciencedirect.com/science/article/pii/S0168900219315694>
- [34] S. Heil, S. Paschalis and M. Petri, On the self-calibration capabilities of γ -ray energy tracking arrays, The European Physical Journal A 54 (10) (2018) 172. doi:10.1140/epja/i2018-12609-0.
URL <https://doi.org/10.1140/epja/i2018-12609-0>
- [35] Mikael Andersson and Torbjörn Bäck, Gamma-ray track reconstruction using graph neural networks, Nuclear Instruments and Methods in Physics Research Section A: Accelerators, Spectrometers, Detectors and Associated Equipment 1048 (2023) 168000. doi:<https://doi.org/10.1016/j.nima.2022.168000>.
URL <https://www.sciencedirect.com/science/article/pii/S016890022201292X>
- [36] A. Gadea et al., Conceptual design and infrastructure for the installation of the first agata sub-array at lnl, Nuclear Instruments and Methods in Physics Research Section A: Accelerators, Spectrometers, Detectors and Associated Equipment 654 (1) (2011) 88 – 96. doi:<https://doi.org/10.1016/j.nima.2011.06.004>.
URL <http://www.sciencedirect.com/science/article/pii/S0168900211011132>

- [37] N. Lalović et al., Performance of the {AGATA} γ -ray spectrometer in the prespec set-up at {GSI}, Nuclear Instruments and Methods in Physics Research Section A: Accelerators, Spectrometers, Detectors and Associated Equipment 806 (2016) 258 – 266. doi:<http://dx.doi.org/10.1016/j.nima.2015.10.032>.
URL <http://www.sciencedirect.com/science/article/pii/S0168900215012395>
- [38] E. Clément, J. Ljungvall, R. M. Pérez-Vidal, J. Dudouet and L. Ménager, On the agata performances at low γ -ray energies, Submitted to NIM A.
- [39] C.E. Lehner, Zhong He and G.F. Knoll, Intelligent gamma-ray spectroscopy using 3-d position-sensitive detectors, IEEE Transactions on Nuclear Science 50 (4) (2003) 1090–1097. doi:10.1109/TNS.2003.814583.
- [40] F.C.L. Crespi et al., Response of agata segmented hpge detectors to gamma rays up to 15.1 mev, Nuclear Instruments and Methods in Physics Research Section A: Accelerators, Spectrometers, Detectors and Associated Equipment 705 (2013) 47, accepted 13 December 2012, Available online 19 December 2012. doi:10.1016/j.nima.2012.12.084.
URL <https://linkinghub.elsevier.com/retrieve/pii/S0168900212016324>
- [41] B. Million et al., Measurement of 15 mev γ -rays with the ge cluster detectors of euroball, Nuclear Instruments and Methods in Physics Research Section A: Accelerators, Spectrometers, Detectors and Associated Equipment 452 (3) (2000) 422–430. doi:[https://doi.org/10.1016/S0168-9002\(00\)00444-7](https://doi.org/10.1016/S0168-9002(00)00444-7).
URL <https://www.sciencedirect.com/science/article/pii/S0168900200004447>
- [42] M. Ciemala et al., Measurements of high-energy γ -rays with labr3:ce detectors, Nuclear Instruments and Methods in Physics Research Section A: Accelerators, Spectrometers, Detectors and Associated Equipment 608 (1) (2009) 76–79. doi:<https://doi.org/10.1016/j.nima.2009.06.019>.
URL <https://www.sciencedirect.com/science/article/pii/S0168900209012170>
- [43] A.M. Stefanini et al., The heavy-ion magnetic spectrometer prisma, Nuclear Physics A 701 (1) (2002) 217 – 221, 5th International Conference on Radioactive Nuclear Beams. doi:[https://doi.org/10.1016/S0375-9474\(01\)01578-0](https://doi.org/10.1016/S0375-9474(01)01578-0).
URL <http://www.sciencedirect.com/science/article/pii/S0375947401015780>
- [44] M. Rejmund et al., Performance of the improved larger acceptance spectrometer: Vamos++, Nuclear Instruments and Methods in Physics Research Section A: Accelerators, Spectrometers,

- Detectors and Associated Equipment 646 (1) (2011) 184 – 191.
doi:<http://dx.doi.org/10.1016/j.nima.2011.05.007>.
URL <http://www.sciencedirect.com/science/article/pii/S0168900211008515>
- [45] J.N. Scheurer et al., Improvements in the in-beam γ -ray spectroscopy provided by an ancillary detector coupled to a ge γ -spectrometer: the diamant-eurogam ii example, Nuclear Instruments and Methods in Physics Research Section A: Accelerators, Spectrometers, Detectors and Associated Equipment 385 (3) (1997) 501 – 510.
doi:[https://doi.org/10.1016/S0168-9002\(96\)01038-8](https://doi.org/10.1016/S0168-9002(96)01038-8).
URL <http://www.sciencedirect.com/science/article/pii/S0168900296010388>
- [46] J.J. Valiente-Dobón et al., Neda-neutron detector array, Nuclear Instruments and Methods in Physics Research Section A: Accelerators, Spectrometers, Detectors and Associated Equipment 927 (2019) 81 – 86.
doi:<https://doi.org/10.1016/j.nima.2019.02.021>.
URL <http://www.sciencedirect.com/science/article/pii/S0168900219301962>
- [47] M. Assié et al., The mugast-agata-vamos campaign: Set-up and performances, Nuclear Instruments and Methods in Physics Research Section A: Accelerators, Spectrometers, Detectors and Associated Equipment 1014 (2021) 165743. doi:<https://doi.org/10.1016/j.nima.2021.165743>.
URL <https://www.sciencedirect.com/science/article/pii/S0168900221007282>
- [48] C. Domingo-Pardo, D. Bazzacco, P. Doornenbal, E. Farnea, A. Gadea, J. Gerl and H.J. Wollersheim, Conceptual design and performance study for the first implementation of agata at the in-flight rib facility of gsi, Nuclear Instruments and Methods in Physics Research Section A: Accelerators, Spectrometers, Detectors and Associated Equipment 694 (2012) 297–312. doi:<https://doi.org/10.1016/j.nima.2012.08.039>.
URL <https://www.sciencedirect.com/science/article/pii/S0168900212009102>
- [49] E. Clément et al., Conceptual design of the agata 1π array at ganil, Nuclear Instruments and Methods in Physics Research Section A: Accelerators, Spectrometers, Detectors and Associated Equipment 855 (Supplement C) (2017) 1 – 12. doi:<https://doi.org/10.1016/j.nima.2017.02.063>.
URL <http://www.sciencedirect.com/science/article/pii/S0168900217302590>
- [50] Francesco Recchia and Caterina Michelagnoli, State-of-the-Art Gamma-Ray Spectrometers for In-Beam Measurements, Springer International Publishing, Cham, 2022, pp. 181–207. doi:10.1007/978-3-031-10751-1_5.

- [51] A. Bracco, F. C. L. Crespi and E. G. Lanza, Gamma decay of pygmy states from inelastic scattering of ions, *The European Physical Journal A* 51 (2015) 99, published: 2015-08-17. doi:10.1140/epja/i2015-15099-6. URL <http://link.springer.com/10.1140/epja/i2015-15099-6>
- [52] D. Mengoni, Ph.D. thesis, University of Camerino (2007).
- [53] A. Lemasson, J. Dudouet, M. Rejmund, J. Ljungvall, A. Grgeren and W. Kortzen, Advancements of γ -ray spectroscopy of isotopically identified fission fragments with agata and vamos++, *EPJ A*.
- [54] A. Gadea et al., Transfer reaction review chapter (2023).
- [55] F. Recchia et al., Position resolution of the prototype agata triple-cluster detector from an in-beam experiment, *Nuclear Instruments and Methods in Physics Research Section A: Accelerators, Spectrometers, Detectors and Associated Equipment* 604 (3) (2009) 555–562. doi:<https://doi.org/10.1016/j.nima.2009.02.042>. URL <https://www.sciencedirect.com/science/article/pii/S0168900209004124>
- [56] H.J. Wollersheim et al., Rare isotopes investigation at gsi (rising) using gamma-ray spectroscopy at relativistic energies, *Nuclear Instruments and Methods in Physics Research Section A: Accelerators, Spectrometers, Detectors and Associated Equipment* 537 (3) (2005) 637–657. doi:<https://doi.org/10.1016/j.nima.2004.08.072>. URL <https://www.sciencedirect.com/science/article/pii/S0168900204019588>
- [57] J. R. Beene et al., Heavy-ion excitation and photon decay of giant resonances in ^{208}Pb , *Phys. Rev. C* 39 (1989) 1307–1319. doi:10.1103/PhysRevC.39.1307. URL <https://link.aps.org/doi/10.1103/PhysRevC.39.1307>
- [58] G. R. Satchler, *Direct Nuclear Reactions*, The International Series of Monographs on Physics, Oxford University Press.
- [59] B. Alikhani et al., Compton polarimetry with a 36-fold segmented hpge-detector of the agata-type, *Nuclear Instruments and Methods in Physics Research Section A: Accelerators, Spectrometers, Detectors and Associated Equipment* 675 (2012) 144–154. doi:<https://doi.org/10.1016/j.nima.2012.02.016>. URL <https://www.sciencedirect.com/science/article/pii/S016890021200174X>
- [60] S. Tashenov, Circular polarimetry with gamma-ray tracking detectors, *Nuclear Instruments and Methods in Physics Research Section A: Accelerators, Spectrometers, Detectors and Associated Equipment* 640 (1) (2011) 164–169. doi:<https://doi.org/10.1016/j.nima.2011.03.011>.

- URL <https://www.sciencedirect.com/science/article/pii/S0168900211005444>
- [61] P. G. Bizzeti et al., Analyzing power of agata triple clusters for gamma-ray linear polarization, *The European Physical Journal A* 51 (4) (2015) 49. doi:[10.1140/epja/i2015-15049-4](https://doi.org/10.1140/epja/i2015-15049-4). URL <https://doi.org/10.1140/epja/i2015-15049-4>
- [62] C. Stahl, N. Pietralla, G. Rainovski and M. Reese, Coulex-multipolarimetry with relativistic heavy-ion beams, *Nuclear Instruments and Methods in Physics Research Section A: Accelerators, Spectrometers, Detectors and Associated Equipment* 770 (2015) 123–130. doi:<https://doi.org/10.1016/j.nima.2014.10.024>. URL <https://www.sciencedirect.com/science/article/pii/S0168900214011711>
- [63] P. Napiralla et al., Benchmarking the prespec@gsi experiment for coulex-multipolarimetry on the $\pi(p_{3/2}) \rightarrow \pi(p_{1/2})$ spin-flip transition in ^{85}Br , *The European Physical Journal A* 56 (2020) 147, published: 2020-05-25. doi:[10.1140/epja/s10050-020-00148-2](https://doi.org/10.1140/epja/s10050-020-00148-2). URL <https://link.springer.com/10.1140/epja/s10050-020-00148-2>
- [64] J. Simpson, The euroball spectrometer, *Zeitschrift für Physik A Hadrons and Nuclei* 358 (2) (1997) 139–143. doi:[10.1007/s002180050290](https://doi.org/10.1007/s002180050290). URL <http://dx.doi.org/10.1007/s002180050290>
- [65] J. Ljungvall and J. Nyberg, A study of fast neutron interactions in high-purity germanium detectors, *Nuclear Instruments and Methods in Physics Research Section A: Accelerators, Spectrometers, Detectors and Associated Equipment* 546 (3) (2005) 553–573. doi:<https://doi.org/10.1016/j.nima.2005.03.122>. URL <https://www.sciencedirect.com/science/article/pii/S0168900205008338>
- [66] J. Ljungvall and J. Nyberg, Neutron interactions in agata and their influence on γ -ray tracking, *Nuclear Instruments and Methods in Physics Research Section A: Accelerators, Spectrometers, Detectors and Associated Equipment* 550 (1) (2005) 379 – 391. doi:<https://doi.org/10.1016/j.nima.2005.04.084>. URL <http://www.sciencedirect.com/science/article/pii/S0168900205012507>
- [67] A Boston et al., Psa review chapter, *EPJ A*.
- [68] A. Ataç, A. Kaşkaş, S. Akkoyun, M. Şenyiğit, T. Hüyük, S.O. Kara and J. Nyberg, Discrimination of gamma rays due to inelastic neutron scattering in agata, *Nuclear Instruments and Methods in Physics Research Section A: Accelerators, Spectrometers, Detectors and Associated Equipment* 607 (3) (2009) 554–563. doi:<https://doi.org/10.1016/j.nima.2009.05.183>.

- URL <https://www.sciencedirect.com/science/article/pii/S0168900209011735>
- [69] M. Şenyiğit et al., Identification and rejection of scattered neutrons in agata, Nuclear Instruments and Methods in Physics Research Section A: Accelerators, Spectrometers, Detectors and Associated Equipment 735 (2014) 267–276. doi:<https://doi.org/10.1016/j.nima.2013.09.035>.
URL <https://www.sciencedirect.com/science/article/pii/S0168900213012692>
- [70] D.G. Jenkins, R. Glover, R.D. Herzberg, A.J. Boston, C. Gray-Jones and A. Nordlund, Proof-of-principle for fast neutron detection with advanced tracking arrays of highly segmented germanium detectors, Nuclear Instruments and Methods in Physics Research Section A: Accelerators, Spectrometers, Detectors and Associated Equipment 602 (2) (2009) 457–460. doi:<https://doi.org/10.1016/j.nima.2009.01.171>.
URL <https://www.sciencedirect.com/science/article/pii/S0168900209002952>
- [71] J van der Marel and B Cederwall, Collimatorless imaging of gamma rays with help of gamma-ray tracking, Nuclear Instruments and Methods in Physics Research Section A: Accelerators, Spectrometers, Detectors and Associated Equipment 471 (1) (2001) 276–280, imaging 2000. doi:[https://doi.org/10.1016/S0168-9002\(01\)01007-5](https://doi.org/10.1016/S0168-9002(01)01007-5).
URL <https://www.sciencedirect.com/science/article/pii/S0168900201010075>
- [72] J. Gerl, Gamma-ray imaging exploiting the compton effect, Nuclear Physics A 752 (2005) 688–695, proceedings of the 22nd International Nuclear Physics Conference (Part 2). doi:<https://doi.org/10.1016/j.nuclphysa.2005.02.068>.
URL <https://www.sciencedirect.com/science/article/pii/S0375947405002277>
- [73] S Moon et al., Compton imaging with AGATA and SmartPET for DESPEC, Journal of Instrumentation 6 (12) (2011) C12048–C12048. doi:10.1088/1748-0221/6/12/c12048.
URL <https://doi.org/10.1088/1748-0221/6/12/c12048>
- [74] T. Steinbach et al., Compton imaging with a highly-segmented, position-sensitive hpge detector, The European Physical Journal A 53 (2) (2017) 23. doi:10.1140/epja/i2017-12214-9.
URL <https://doi.org/10.1140/epja/i2017-12214-9>
- [75] M. Doncel, F. Recchia, B. Quintana, A. Gadea and E. Farnea, Experimental test of the background rejection, through imaging capability, of a highly segmented agata germanium detector, Nuclear Instruments and Methods in Physics Research Section A: Accelerators, Spectrometers, Detectors and Associated Equipment 622 (3) (2010) 614–618.

doi:<https://doi.org/10.1016/j.nima.2010.07.069>.

URL <https://www.sciencedirect.com/science/article/pii/S0168900210016839>

- [76] S.J. Wilderman, W.L. Rogers, G.F. Knoll and J.C. Engdahl, Fast algorithm for list mode back-projection of compton scatter camera data, IEEE Transactions on Nuclear Science 45 (3) (1998) 957–962. doi: 10.1109/23.682685.